



저작자표시-비영리-변경금지 2.0 대한민국

이용자는 아래의 조건을 따르는 경우에 한하여 자유롭게

- 이 저작물을 복제, 배포, 전송, 전시, 공연 및 방송할 수 있습니다.

다음과 같은 조건을 따라야 합니다:



저작자표시. 귀하는 원저작자를 표시하여야 합니다.



비영리. 귀하는 이 저작물을 영리 목적으로 이용할 수 없습니다.



변경금지. 귀하는 이 저작물을 개작, 변형 또는 가공할 수 없습니다.

- 귀하는, 이 저작물의 재이용이나 배포의 경우, 이 저작물에 적용된 이용허락조건을 명확하게 나타내어야 합니다.
- 저작권자로부터 별도의 허가를 받으면 이러한 조건들은 적용되지 않습니다.

저작권법에 따른 이용자의 권리는 위의 내용에 의하여 영향을 받지 않습니다.

이것은 [이용허락규약\(Legal Code\)](#)을 이해하기 쉽게 요약한 것입니다.

[Disclaimer](#)

공학석사학위논문

**Synthesis of polymer binder based on phenanthrene  
for Si anode via Suzuki polycondensation**

스즈키 폴리컨덴세이션을 통한 실리콘 음극을 위한  
페난쓰렌 기반의 폴리머 바인더의 합성

2014年 8月

서울대학교 대학원

화학생물공학부

최 성 열

# Synthesis of polymer binder based on phenanthrene for Si anode via Suzuki polycondensation

스즈키 폴리컨덴세이션을 통한 실리콘 음극을 위한  
페난쓰렌 기반의 폴리머 바인더의 합성

指導教授 : 金 榮 奎

이 論文을 工學碩士 學位論文으로 提出함

2014年 8月

서울大學校 大學院

化學生物工學部

崔 誠 烈

崔 誠 烈의 工學碩士 學位論文을 認准함

2014年 6月

委員長 \_\_\_\_\_ (印)

副委員長 \_\_\_\_\_ (印)

委 員 \_\_\_\_\_ (印)

**Synthesis of polymer binder based on phenanthrene  
for Si anode via Suzuki polycondensation**

By  
SungYeol Choi

August 2014

Thesis Adviser: Young Gyu Kim

# ABSTRACT

Recently, the demand for next generation LIBs which is required for high capacity such as EV (Electrical vehicle), ESS (electrical storage system) have been ever increasing. Due to this trend, a number of studies have focused on the Si, Si alloy, Nano structuring Si as promising negative materials which has high theoretical capacity of electrochemical lithiation compared to currently commercialized graphite. However, although so many breakthrough for commercializing Si anode, high capacity Si anode still cannot be commercialized due to critical problem, extensive volume changes during charge-discharge cyclings which results in crack or fracture of active materials. So binder material has been found to be a critical factor for enhancing the cyclic performance of anode materials such as silicon and its composites. Therefore, the binder selection is said to be very important in employing high capacity anode materials.

So we developed new polymer binder material which has conductivity. Because if binder has conducting nature, we can use only binder in the electrode without conductive additives conventionally used. It may help to maintain electrochemical cycling with only small amount of binder. We could synthesize 3,6-poly(phenanthrenequinone) successfully through several trials and investigated how well polymer

function as binder as well as conducting agent in nano Si electrode. We could discover synthesized polymer could be functioned as mixed conductor which showed itself some capacity. Through trial to control molecular weight of polymer, it seemed to be controlled by reaction time in modified reaction scheme. According to its electrochemical data, polymer which has approximately  $M_n=100000$  showed better rate capability and cycle life test than the other polymer. It is unexpected results that should need further study. Between  $M_n < 5000$  and  $100000$  polymer, we could know high molecular polymer show better electrochemical performances. Thus new developed polymer gives good electrical contact which is due to its conducting nature. It shows potential binder for the Si electrodes that the conventional conducting agent can be excluded or the amount used can be decreased.

*.Keywords:* lithium ion battery, binder, conducting polymer, Silicon anode,

*Student number:* 2012-20981

# TABLE OF CONTENTS

<b>ABSTRACT</b> .....	4
<b>LIST OF FIGURES</b> .....	8
<b>LIST OF TABLES</b> .....	9
<b>LIST OF SCHEMES</b> .....	10
<b>LIST OF ABBREVIATIONS</b> .....	11
<b>Introduction</b> .....	13
<b>1. Introduction of Lithium ion batteries</b> .....	13
<b>2. Anode</b> .....	15
2.1. Silicon as anode material.....	16
<b>3. Polymer binder</b> .....	18
<b>4. Conducting polymer</b> .....	21
4.1. Doping.....	23
<b>Results &amp; discussion</b> .....	26
<b>1. Initial studies for conductive binder</b> .....	26
1.1. Design of target molecule.....	26

1.2. Synthesis of PPH derivative and its copolymers.....	27
<b>2. Design of modified target polymer and its synthesis.....</b>	<b>30</b>
2.1. Design of new target polymer.....	30
2.2. Synthesis of 3,6-poly(phenanthrenequinone) .....	33
2.3. 3,6-PPQ as mixed conductor.....	34
2.4. Modified synthetic scheme of 3,6-PPQ.....	38
2.5. Electrochemical test with synthesized PPQ.....	40
<b>Experimental Details.....</b>	<b>45</b>
<b>REFERENCES.....</b>	<b>69</b>
<b>ABSTRACT IN KOREAN.....</b>	<b>73</b>



# LIST OF FIGURES

Figure 1. Schematic scheme of Li-ion batt	<b>ABSTRACT</b>
.....	4
<b>LIST OF FIGURES</b>	8
<b>LIST OF TABLES</b>	9
<b>LIST OF SCHEMES</b>	10
<b>LIST OF ABBREVIATIONS</b>	11
<b>Introduction</b>	13
<b>1. Introduction of Lithium ion batteries</b>	13
<b>2. Anode</b>	15
2.1. Silicon as anode material	16
<b>3. Polymer binder</b>	18
<b>4. Conducting polymer</b>	21
4.1. Doping	23
<b>Results &amp; discussion</b>	26
<b>3. Initial studies for conductive binder</b>	26
1.1. Design of target molecule	26

1.2. Synthesis of PPH derivative and its copolymers.....	27
<b>4. Design of modified target polymer and its synthesis.....</b>	<b>30</b>
2.1. Design of new target polymer.....	30
2.2. Synthesis of 3,6-poly(phenanthrenequinone) .....	33
2.3. 3,6-PPQ as mixed conductor.....	34
2.4. Modified synthetic scheme of 3,6-PPQ.....	38
2.5. Electrochemical test with synthesized PPQ.....	40
<b>Experimental Details.....</b>	<b>45</b>
<b>REFERENCES.....</b>	<b>69</b>
<b>ABSTRACT IN KOREAN.....</b>	<b>73</b>
ery .....	13
Figure 2. Theoretical capacity of electrode materials .....	16
Figure 3. Reported polymer binder for Si anode .....	19
Figure 4. Volumic changes during lithiation and delithiation in high capacity anode.....	20
Figure 5. Mechanism of forming conductivity in <i>p</i> -type polymer.....	24
Figure 6. DFT calculation of fluorenone and phenanthrenequinone...	32

Figure 7. Polymer purification .....	35
Figure 8. Evidence of mixed conductor of 3,6-PPQ .....	37
Figure 9. Rate test of Si electrode .....	41
Figure 10. Cycle life test of Si electrode .....	42
Figure 11. Binder contents test.....	43

## **LIST OF TABLES**

Table 1. Common conducting polymers.....	22
Table 2. GPC analysis of synthesized polymers.....	30
Table 3. Screening of deprotection of acetal group.....	34
Table 4. GPC analysis of synthesized polymers.....	36
Table 5. Screening of modification of polymer.....	39
Table 6. GPC results of polymer from 1 to 3 days.....	40
Table 7. The result of cycle life test.....	43

Table 8. The result of binder contents test .....	44
---	----

## LIST OF SCHEMES

Scheme 1. Design of target molecule.....	26
Scheme 2. Retrosynthetic analysis of target molecule.....	27
Scheme 3. Synthesis of monomers.....	28
Scheme 4. Synthesis of poly(phenanthrene) derivatives.....	29
Scheme 5. Copolymerization.....	29
Scheme 6. Reported polyfluorene for binder and proposed polymer...31	
Scheme 7. Proposed mechanism of electro-reduction of PQ.....	32

Scheme 8. Synthesis of 3,6-dioxaborolane $\alpha$ -diketone compound....	33
Scheme 9. The difference of conversion by reaction concentration...	34
Scheme 11. Polymerization of 3,6-PPQ .....	35
Scheme 12. N-doping mechanism of 3,6-PPQ .....	37
Scheme 13. The effect of Pd catalyst in polymerization and borylation .....	38
Scheme 14. Modified polymerization scheme .....	39

# LIST OF ABBREVIATIONS

d	Doublet
dd	doublet of doublet
CMC	Carboxymethyl cellulose
h	hour(s)
Hz	Hertz
<i>J</i>	coupling constant(s)
LIB	lithium ion battery
M	mole(s) per liter
m	Multiplet
MW	Molecular weight
NMR	nuclear magnetic resonance spectroscopy
PPH	Poly(phenanthrene)
PPQ	Poly(phenanthrenequinone)
PQ	Phenanthrenequinone
q	Quartet
quant.	Quantitative
RT	room temperature
s	Singlet
SEI	solid electrolyte interphase
SPC	Suzuki polycondensation

T	Temperature
t	Time
<i>t</i>	Triplet
TLC	Thin layer chromatography
THF	Tetrahydrofuran
PAA	Poly(acrylate)
NMP	<i>N</i> -methyl-2-pyrrolidone

# Introduction

## 1. Introduction of Li-ion battery

The inevitable depletion of non-renewable fossil fuels and environmental issues, such as CO<sub>2</sub> emissions and thawing of the glacial force us to give away from using fossil fuels as the main global energy source. Green energy sources, such as solar, hydroelectric, thermal and wind energy will finally replace traditional energy sources. Most of these renewable energy sources are especially dependent on the time and surroundings. Electrical energy storage, such as batteries and supercapacitor is very important for us to solve the problems, as they can

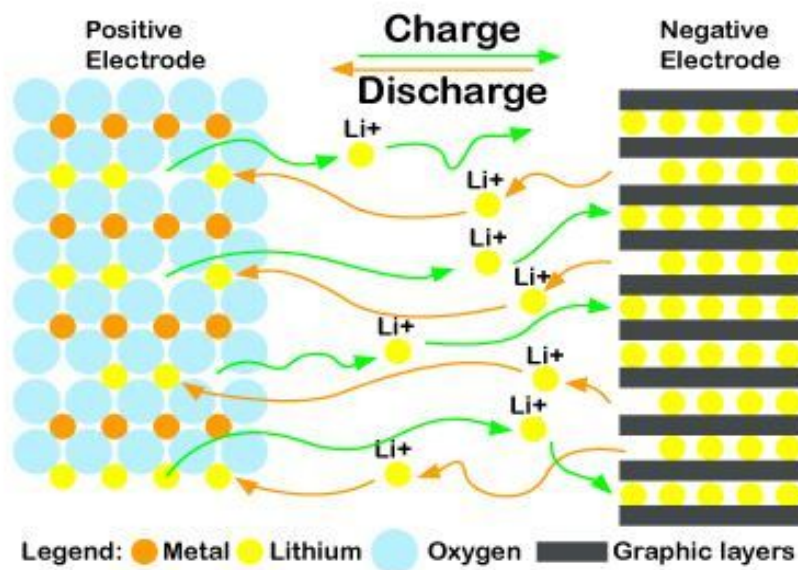


Fig.1) Schematic scheme of Li-ion battery



efficiently store electricity in chemicals and release it when energy demanded.

Current lithium ion battery gives the highest energy density among the rechargeable battery technologies, dominating the market for mobile electronic devices for decades. However, alternative forms of transportation, such as plug-in hybrid electric vehicles (PHEV) and all electric vehicles (EV), require significant improvements in many perspectives, such as energy density, safety, durability and cost. The keys to the success of development of novel and advanced rechargeable batteries are the materials. Demonstrated by Whittingham,  $\text{TiS}_2$  was shown to serve as a host for reversible intercalated and de-intercalated lithium into its structure. <sup>[1]</sup> The single phase behavior during cycling enables it to fully remove and insert lithium ions reversibly. In the 1970s, the discovery of  $\text{TiS}_2$  resulted in Exxon's cells as large as 45 Wh. In the original Exxon  $\text{LiTiS}_2$  batteries, pure lithium served as the anode. The dendritic growth of lithium metal during cycling can short out the cell, which will potentially lead to explosion hazards. In the 1990s, carbonaceous material was discovered as a highly reversible and low voltage Li intercalation–deintercalation anode, as it shows unique properties. Combining safety features of the carbon anode and the high voltage  $\text{LiCoO}_2$  cathode, SONY commercialized the lithium ion battery (C/ $\text{LiCoO}_2$  cell) for the first time, which have dominated the market for electronics so far. Although carbon-

based anodes have the advantage of a long cycle life, low cost and abundant natural resources, low operating potential to Li metal, good electrical conductivity. the graphite anode has significant disadvantages with regards to low gravimetric and volumetric specific capacity (372 mAh/g and 833 mAh/cm<sup>3</sup>). Recently, Lithium–metal alloys, such as lithium–tin have been studied as the most promising materials to replace current carbon-based anodes, because of their high capacity. The recent commercial success of these anodes includes nanostructured SnCo anodes used in SONY’s Nexelion battery, which has a 50% increase in volumetric capacity over the conventional battery.<sup>[2]</sup>

## **2. Anode**

Currently, Li-ion battery consists of carbonaceous graphite negative electrode and LiCoO<sub>2</sub> positive electrode. Graphite, a layered intercalation compound, is one of the most widely used lithium anodes because of necessary advantages that is referred above. Lithium can be readily inserted and extracted into the structure during charge, discharge cycling. When fully lithiated, graphite have stable phases up to the LiC<sub>6</sub> corresponding to a theoretical specific capacity of 372 mAh/g in the electrochemical system.<sup>[3]</sup>

Tin and silicon based materials offer specific capacity values much

higher than conventional graphite. Unfortunately, all of these classes of materials are generally in trouble in large volume expansion during lithiation, which generates enormous mechanical stress and pulverizes the electrode during the charge/discharge cycles. Recent researchers afford new breakthrough by introducing several types of Si material by changing chemical physical properties.

## 2.1. Silicon as anode material

In the previous battery development, most of the trend has been focused on the portable electronic devices which was made with high energy density materials. Recently, the demand for next generation LIBs which

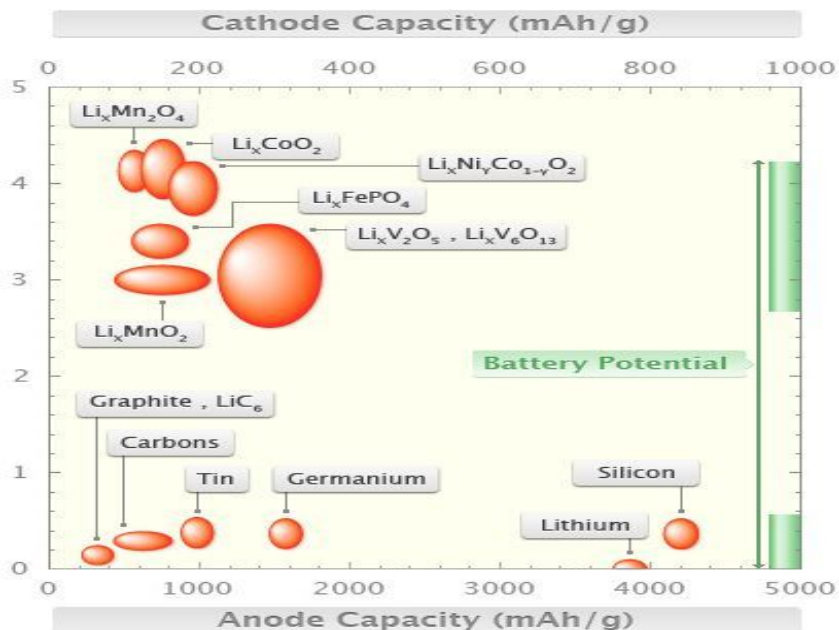


Fig.2) Theoretical capacity of electrode materials

is required for EV (electrical storage system), ESS (electrical storage system) have been ever increasing. So recently, the researchers have widely studied silicon as promising negative materials which has high theoretical capacity of electrochemical lithiation. Silicon possesses a very high theoretical capacity of 4200 mAh/g which correspond to fully lithiated state of  $\text{Li}_{22}\text{Si}_5$  (4.4 Li per Si),  $\text{Li}_{15}\text{Si}_4$  at room temperature (3.6 Li per Si) <sup>[4]</sup> which has a maximum theoretical capacity of 3579 mAh g<sup>-1</sup>.

Unfortunately, similar to tin anode, commercialization of Si as negative electrode have been quite troublesome due to some critical problems which has large volume changes during Li insertion and extraction. A volume expansion of 400% occurs upon insertion and extraction of lithium during cycling. <sup>[5]</sup> This is almost one of the highest volume expansions among the common alloy anodes. Thus, very high irreversible capacity in the first cycle and capacity fading of subsequent cycles were observed for the micron size silicon. Therefore, much effort has been devoted to increasing the performance and cyclability of silicon materials.

Synthesized nano-scaled silicon or silicon / carbon composite are among the most effective methods. Nano-sized silicon showed superior performance to micron sized silicon. Li *et al.* reported that decreasing the silicon particle size to the nanometer-scale (78 nm) can be achieved by laser-induced silane gas reaction. <sup>[7]</sup> By controlling the voltage range between 0 to 0.8 V, silicon nano powder anode showed a reversible

capacity of 1700 mAh/g after 15 cycles. Due to the smaller volume changes by the distribution of nanoparticles, better capacity retention than normal Si powder (passed through 250 meshes) was observed. Cycling at a current density of 0.8 mA/cm<sup>2</sup>, the nano-silicon anode remained at a high capacity of 1500 mAh/g.

Another one is forming composite materials in which active alloy or metal particles are finely dispersed in an active or inactive solid matrix which buffers the expansion of the active phase. However, this effect is not long lasting. So that the capacity is solely maintained for a few tens of cycles. The last one relies on thin films technologies which take advantage of the constraints inherent to the grown Si films to partially maintain the electrode cohesion with the end result being an good capacity retention but an overall capacity limited by the back substrate dead weight.

## **5. Polymer binder**

In LIBs, binder systems are composed of polymeric materials that is used either to bind active material or between active material and current collectors to provide electrical performances in electrodes. The binder in general is electrochemically inert. However, the importance of binders has recently been increased because the binder material was found to be a

critical factor for enhancing the cyclic performance of anode materials such as silicon and its composites.

Recent researches on binders has focused on modified conventional PVdF and CMC materials, copolymerizing PVdF with an elastomeric fluorine polymer <sup>[10]</sup>, the amount of metal salts in CMC <sup>[11]</sup>, Alginic acid,

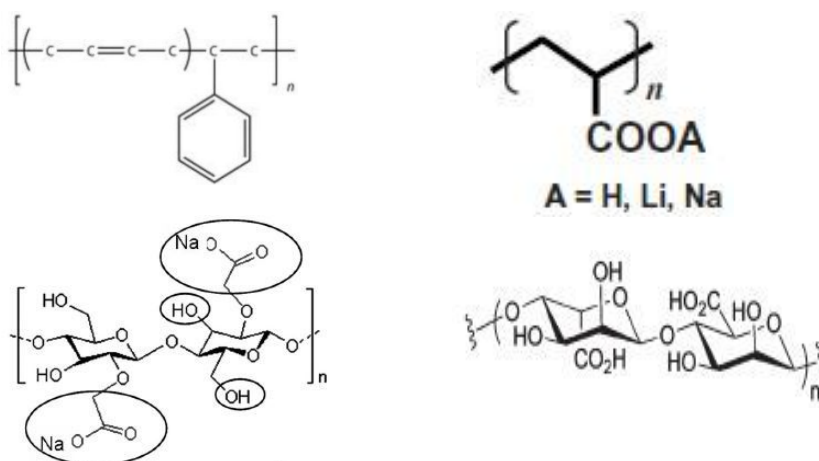


Fig. 3) Reported polymer binder for Si anode

which exhibits excellent binder properties, is also regarded as a CMC derivative. <sup>[8]</sup> On top of them, a number of polymers have recently been examined as potential binder for anode materials, including polyacrylic acid, polyvinyl alcohol, polyacrylate and polyamide imide. These polymers form strong hydrogen bonds with both active materials and current collectors due to functional groups such as hydroxyl and carboxylic acid groups. This leads to enhanced cyclic retention during the charge/discharge processes. But there are some limitations for

commercializing these binders for negative electrode. Because extensive amount of conductive additives and polymer binder should be used. More importantly, these polymer binder still cannot accommodate volumic changes of Si particles.

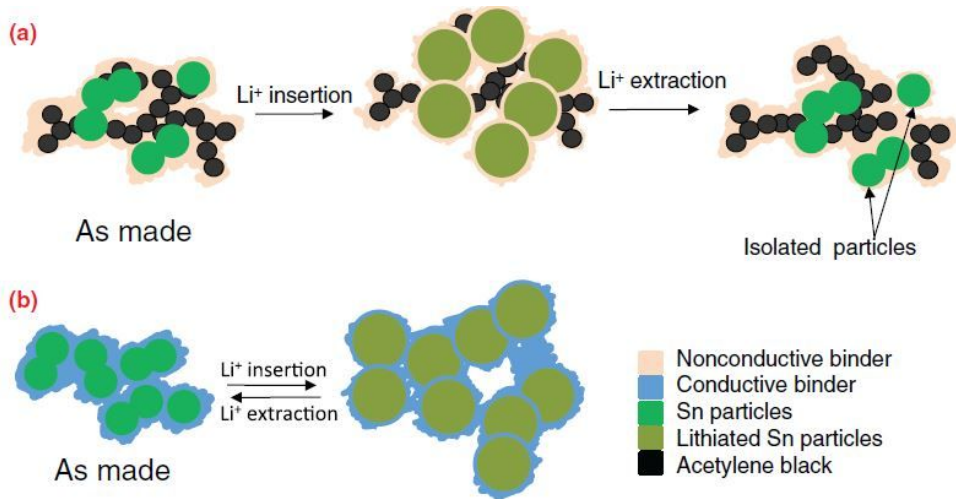


Fig.4) Volumic changes during lithiation and delithiation  
in high capacity anode <sup>[5]</sup>

In contrast to graphite, silicon must be regarded as a conversion material. This means that lithium insertion does not occur as an intercalation reaction but rather as a conversion reaction comprising breakup and reorganization of the silicon lattice upon alloying with lithium. The volumic changes which was caused by accommodation of lithium ions result in the cracks / fractures of the particles in the composite electrode of the particle, exfoliation of the composite from current collector. This

volumic changes during the operation causes significant challenges in selecting the binder, which holds the active material together in the anode of LIBs.

Thus, we tried to developed new polymer binder which has conductivity for approaches to overcome the adverse effects of the volume change in high-capacity electrodes there is no need to use conductive additives which means polymer can function both binder and conducting additives, which is satisfied with cyclings with small amount of polymer. We just focused on the conducting nature and its electrochemical performances in this thesis even if binder should be satisfied with physical properties. So further studies for enhancing mechanical properties is required.

## **4. Conducting polymer**

Polymers have long been used as insulating materials. There are four classes of conjugated polymers that have been developed so far. They include conjugated conducting polymers, charge transfer polymers, ionically conducting polymers and conductively filled polymers. We mostly focused on the conjugated conducting polymers which has conductivity in the electrochemical system.

Owing to the delocalization of electrons in a continuously overlapped p-orbital along the polymer backbone, conjugated polymers possess



interesting optical and magnetic properties. These unusual optoelectronic properties allow conjugated polymers to be used for a large number of applications, including protecting metals from corrosion, sensing devices, artificial actuators, all-plastic transistors, non-linear optical devices and light-emitting displays. However, owing to the backbone rigidity intrinsically associated with the delocalized conjugated structure, most unfunctionalized conjugated polymers are intractable (insoluble and brittle).

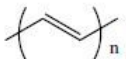
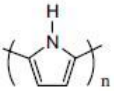
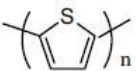
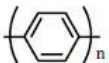
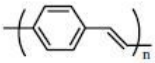
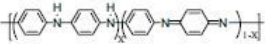
Polymer (date conductivity discovered)	Structure	•••• gap (eV)	Conductivity <sup>#</sup> (S/cm)
I. Polyacetylene and analogues			
Polyacetylene (1977)		1.5	$10^3 - 1.7 \times 10^5$
Polypyrrole (1979)		3.1	$10^2 - 7.5 \times 10^3$
Polythiophene (1981)		2.0	$10 - 10^3$
II. Polyphenylene and analogues			
Poly(paraphenylene) (1979)		3.0	$10^2 - 10^3$
Poly(p-phenylene vinylene) (1979)		2.5	$3 - 5 \times 10^3$
Polyaniline (1980)		3.2	30 - 200

Table. 1) Common conducting polymers

the conjugated structure with alternating single and double bonds providing  $p$ -orbitals for a continuous orbital overlap seems to be necessary for polymers to become conducting. This is because just as metals have high conductivity due to the free movement of electrons through their structure, in order for polymers to be electronically conductive they must possess.

#### 4.1. Doping

The band theory can provide some information about the doping induced changes in electronic structure and the way in which charges can be stabilized on the polymer chains and the nature of the charge transport process are still ambiguous. The electrical properties of direct gap inorganic semiconductors are determined by their electronic structures, and the electrons move energy states called bands. The bonding and antibonding  $p$ -orbitals of the  $sp^2$  hybridized electron materials generate energy bands, which are fully occupied and empty. The highest occupied band is called the valence band, and the lowest unoccupied band is the conduction band. The energy difference between them is called the band gap. Electrons must have certain energy to occupy a given band and need additional energy to move from the valence band to the conduction band. semiconductors, however, in the case of conjugated polymers have

narrower band gaps which doping can be easily conducted and change their band structures by either taking electrons from the valence band (p-doping) or adding electrons to the conduction band (n-doping).

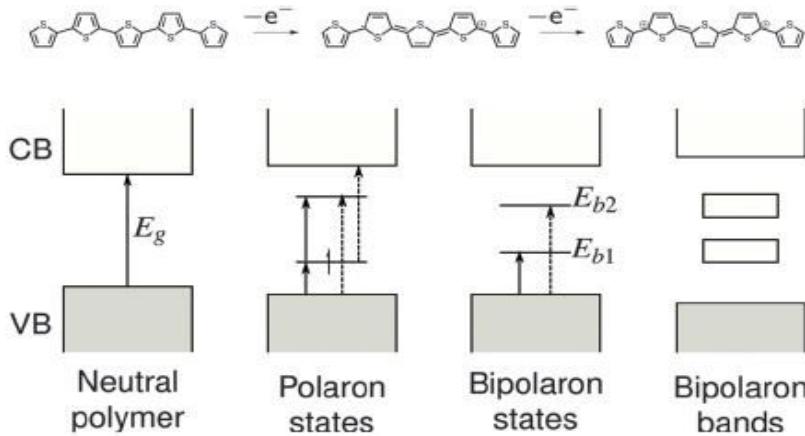


Fig.5) Mechanism of forming conductivity in p-type polymer

For example, in p-type polymer such as poly(thiophene), When an electron is removed from the top of the valence band of a conjugated polymer the valence band ends up being partially filled and a radical cation, commonly termed as a polaron, is formed. The formation of polarons causes the injection of states from the bottom of the conduction band and top of the valence band into the band gap. A polaron carries both spin and charge. Removal of a second electron on a chain already having a positive polaron results in the formation of a bipolaron through dimerization of two polarons, which can lower the total energy. In conjugated polymers with a degenerate ground state, the population of polarons and bipolarons increases with the doping level. At high doping levels, the localized polarons, bipolarons near to individual dopant ions

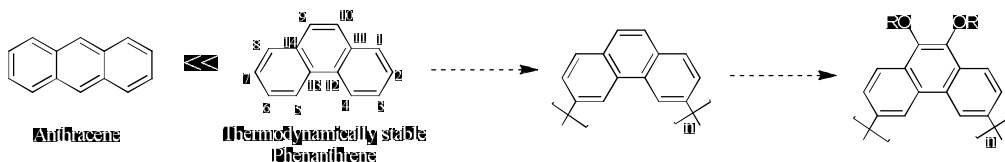
could overlap, leading to new energy bands between and even overlapping the valence and conduction bands, through which electrons can flow.

# Results and Discussion

## 1. Initial studies for conducting binder

### 1.1. Design of target molecule

Recently, polycyclic aromatic hydrocarbons such as phenanthrene (Ph) have been investigated numerically and theoretically due to its importance as electrode materials for Li-ion rechargeable batteries. Ph is the simplest aromatic hydrocarbons, thermodynamically stable and a promising block for building  $\pi$ -conjugated conducting polymers.

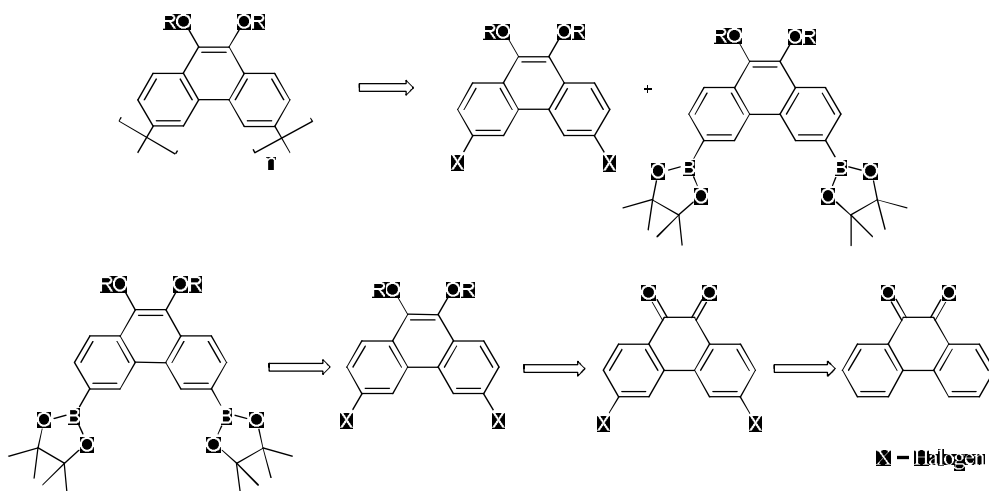


Sch. 1) Design of target molecule

So we determined that the prototype of target polymer is based on phenanthrene backbone, polyphenanthrene (PPh) which is expected that PPh show higher conductivity due to long conjugation length and can be easily n-doped under voltage range of lithiation and delithiation cycling in the Si anode because of low LUMO value resulting from long conjugation length. Additionally, target polymer also should be satisfied with mechanical properties in the anode system. Thus we introduce ether alkyl

chain at 9,10–position of phenanthrene for enhanced mechanical properties.

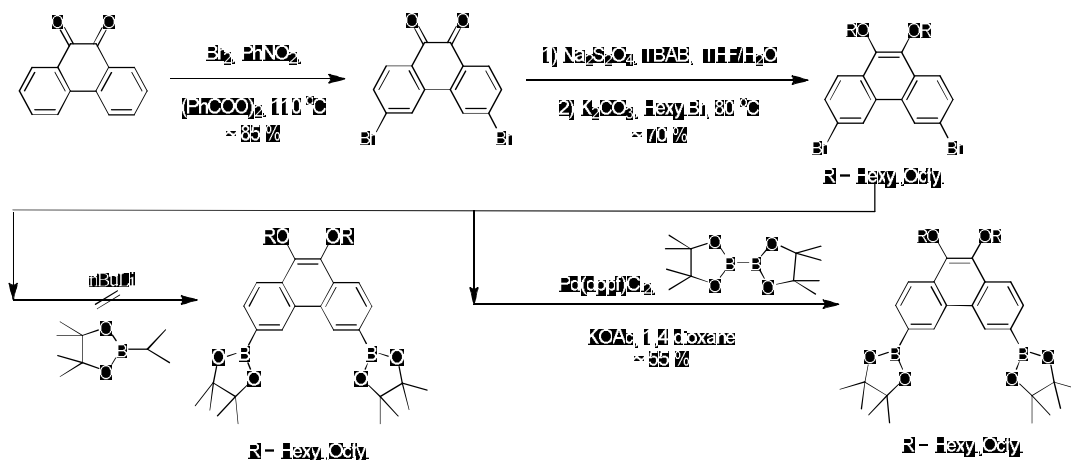
Based on them, We conducted retrosynthetic analysis of target polymer.



Sch.2) Retrosynthetic analysis of target molecule

We synthesized poly(phenanthrene) derivative via Suzuki cross coupling. So we should prepare two types of monomer, dihalo and dioxaborolane compound. Dioxaborolane compound can be synthesized from 9,10-phenanthrenequinone. The other monomers also can be synthesized from same starting material, which is advantageous. So we planned to synthesize polymer depicted on upper synthetic scheme

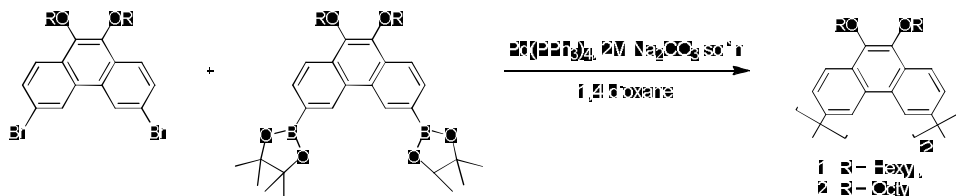
## 1.2. Synthesis of PPh derivative and its copolymers



Sch.3) Synthesis of monomers

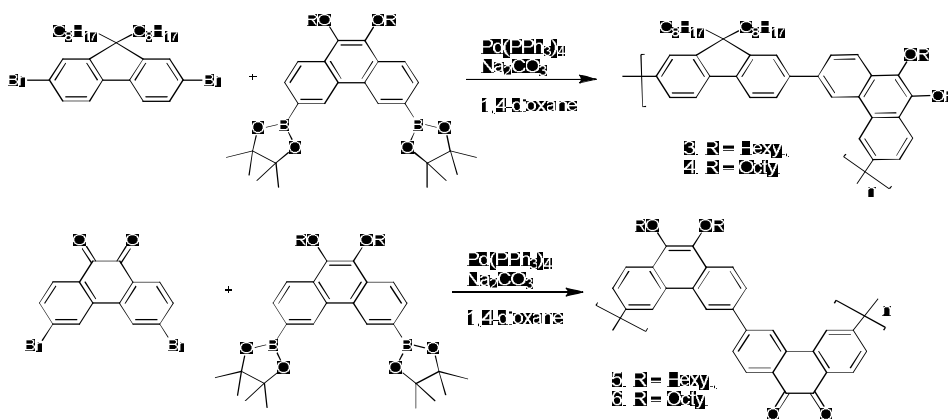
We could synthesize dibromo compound which was reacted selectively at 3,6-position via radical mechanism.<sup>[15]</sup> Following reduction and alkylation was easily conducted to give alkyl ether introduced compound. Next step, miyaura borylation was conducted. Vanormelingen *et al* reported this step was troublesome.<sup>[16]</sup> Generally, the introducing of boronic acid pinacol ester was conducted with *n*-BuLi and isopropoxyboronic acid pinacol ester. After Li-Br exchange, lithiated species were scrambled at high temperature which result in the formation of several region-isomers of borylation product in the process of coupling with boronic ester. So Pd catalyzed reaction which is more mild reaction than compared to conventional synthesis and high regioselective, so called Suzuki miyaura reaction was successfully conducted.<sup>[17]</sup> I also adapted this condition to our substrate to give desired product with 55 % yield. Finally,

polymerization <sup>[16,18]</sup> was conducted under Suzuki reaction with prepared monomers.



Sch.4) Synthesis of poly(phenanthrene) derivative

And homopolymerization as well as copolymerization also conducted. Dioctylfluorene dibromide which was from commercial supplier and prepared dibromo compound was copolymerized with ether chain monomer for enhanced electrochemical activity.



Sch.5) Copolymerization

So molecular weight of their synthesized polymers was measured by gel permeation chromatography (GPC, THF solvent PS standard)



Compound	$M_n$	$M_w$	$M_w / M_n$
1	5445	13311	2.445
2	4192	6304	1.504
3	5510	9233	1.676
4	4177	6747	1.615
5	1953	3091	1.583
6	3978	9845	2.479

Table. 2) GPC analysis of synthesized polymers

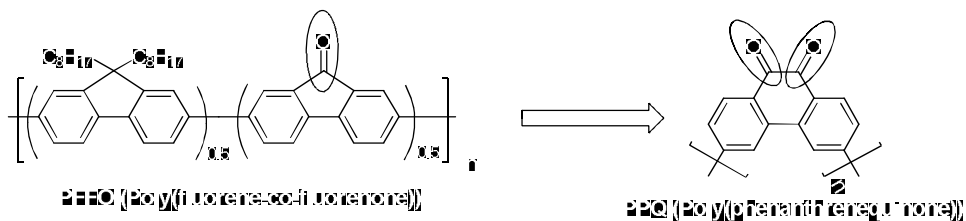
Unfortunately, all synthesized polymers did not show electrochemical activity by testing cyclic voltammetry and charge-discharge test with  $\text{SiO}_x$  as active material. Definitely, they did not seem to show reduction peak in the reactive voltage potential of Si (0 ~ 1 V) that means polymers did not carry electrons and Li ion. So the requirement for conducting polymer should be reduced in the voltage range of 0 ~ 1 V in order to show conductivity.

## 2. Design of modified polymer and its synthesis

### 2.1. Design of new target polymer

Recently, the polyfluorene type of conductive polymer binder for Si anode was reported.<sup>[9a, 9b]</sup> In this paper the carbonyl group of polymer binder function as electrochemically active site where Li ion can bind to give

electronic conductivity. Based on this concept, we planned to modify polymer structure for reacting in the fulfilled voltage range of Si anode.



Sch.6) Reported polyfluorene for binder and proposed polymer

We chose the poly(phenanthrenequinone) (PPQ), which has two carbonyl groups which is similar to reported polymer. We conducted DFT (density functional theory) calculation with RB3LYP / 6-31G(d,p) method in Gaussian 09 to compare LUMO energy level with fluorenone. According to the result, LUMO of phenanthrenequinone (PQ) was lower than that of fluorenone. So new quinone type polymer is expected to show more lower LUMO energy level to be able to easily reduced in the Si voltage range. Furthermore, PQ was reported it is good acceptors of electrons which can undergo reversible reduction to produce semiquinone and catechol compound.<sup>[19]</sup> PQ showed two step reduction process which is due to the presence of conjugation ring adjacent to the 9, 10-positions of carbonyl group that provide the stability to the reduced species of PQ.

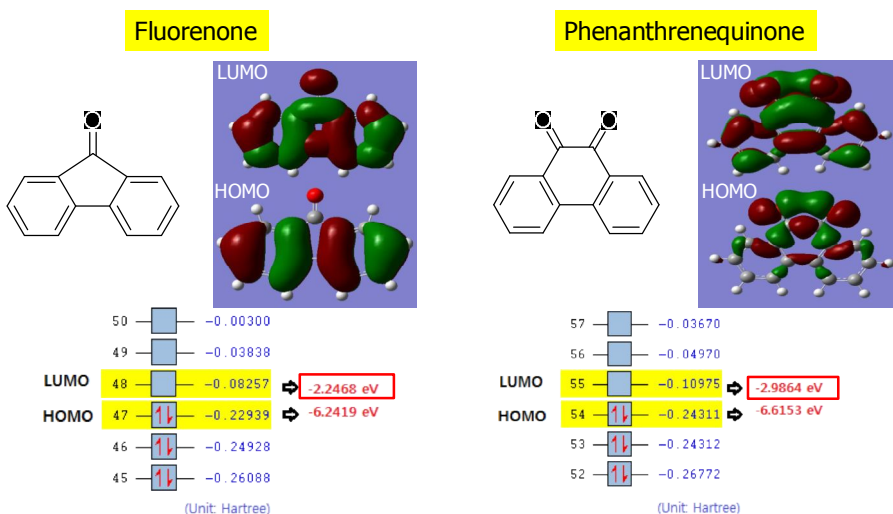
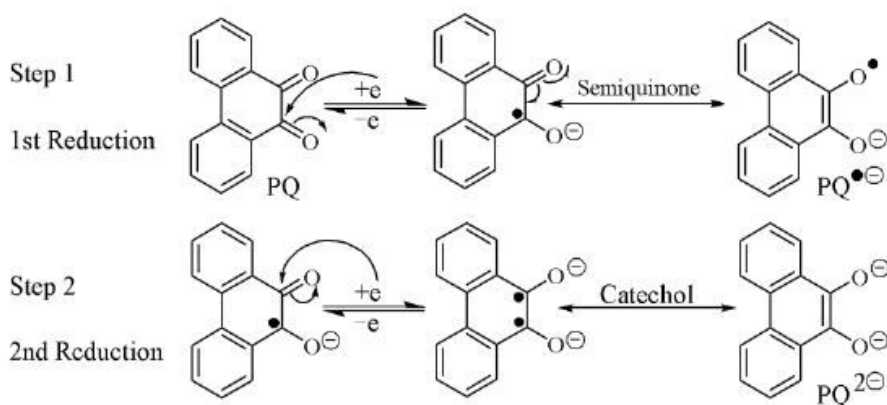


Fig.6) DFT calculation of fluorenone and phenanthrenequinone

respectively. Simplified mechanism of electron-reduction is shown in scheme 7

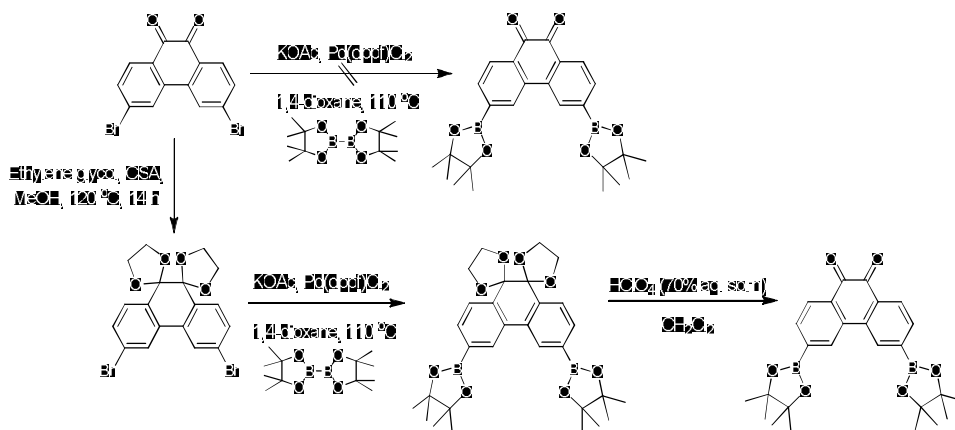


Sch.7) Proposed mechanism of electro-reduction for PQ

So we assume that PQ is more electrochemically active than fluorenone due to the reasons mentioned above. We planned to synthesize PPQ which contain both PQ backbone and quinine group.

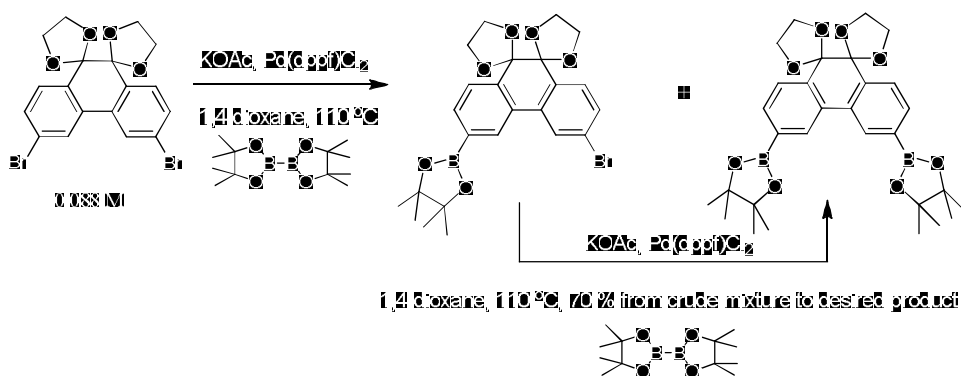
## 2.2. Synthesis of 3,6-poly(phenanthrenequinone)

In order to synthesize PPQ, it was important to activate carbonyl functional group in the polymer structure. So we tried to synthesize oxaborolane compound from dibromo compound.



Sch. 8) Synthesis of 3,6-dioxaborolane  $\alpha$ -diketone compound

However, in spite of several trials, most of starting material were recovered and unidentified side product could be obtained. We assumed that it was because of Pd competition to reactive site to cause Pd deactivation for coupling. This Pd effect was found in the modified synthetic scheme and it will be explained in that part. So we determined to introduce ethylene glycol protection and deprotection of carbonyl group. <sup>[20]</sup> I could obtain acetal protected dibromo compound with 80 ~ 90% yield. And in the following borylation step, monoborylation product could



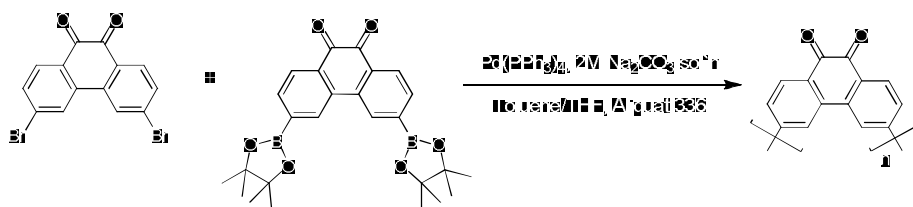
Sch. 9) . The difference of conversion by reaction concentration

sometimes be obtained in the mixture with desired product (mono : di = 1:3 ~ 1:2 ratio). Fortunately, when reaction mixture is three times diluted (0.029 M), I could notice that single spot was formed by monitoring TLC and desired product could be obtained with 65 ~ 74 % yield. As the last step, deprotection of ethylene glycol group could be conducted in the acidic condition. Some trials are shown in the table below.

	Acid	Solvent	Time	Temp	Yield
Entry 1	TsOH	CH <sub>3</sub> CN : DCM = 2:1	24 h	reflux	42 % (with impurity)
Entry 4	HClO <sub>4</sub> (70 % sol'n)	DCM	1 h	0	93 %

Table 3.) Screening of deprotection of acetal group

Deprotection was successfully conducted in the perchloric acid in DCM with high yield during very short time.<sup>[21]</sup> Finally, we could finish preparing two monomers for PPQ which was followed by polymerization under Suzuki condition. Obtained crude polymer was purified through several steps as depicted procedure below. So low molecular weight of oligomers could be removed. And GPC analysis was conducted with obtained polymer powder in PMMA based column in DMF solution.



Sch. 11) Polymerization of 3,6-PPQ

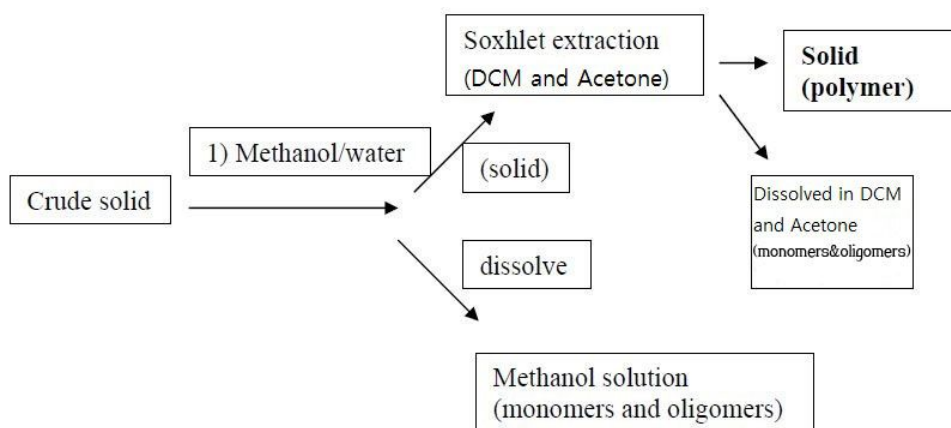


Fig.7 ) Purification of crude polymer

Theoretically, according to the condensation polymerization kinetics, molecular weight of polymer is dependent on the reaction time and

concentration. So higher reaction time is introduced, higher degree of polymerization, in other words, high molecular weight. Because the higher molecular weight, the longer conjugation length. Thus long conjugation length of polymer can lower band gap of HOMO and LUMO which result in the enhanced conductivity. At first, we changed reaction time from 1 to 3 days in order to changes of MW of polymer.

	Reaction time	Concentration	Mn / PDI
Entry 2	2 days	0.012 M	83259 / 1.32
	3 days	0.012 M	63662 / 1.35
Entry 3	1 days	0.012 M	53122 / 1.31
	2 days	0.012 M	58645 / 1.43

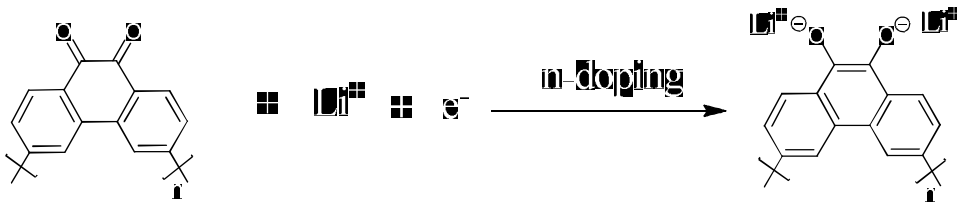
Table 4. ) GPC result of synthesized polymers

In Entry 1, it showed very low MW polymer. Based on the experience of borylation step, I conducted polymerization under 3 times diluted system. Expectedly, MW in entry 2 was higher than that in entry 1.

### 2.3. 3,6-poly(phenanthrenequinone) as mixed conductor

In this period, we discovered that 3,6-PPQ is mixed conductor which means that PPQ can transport electron while binding Li ion. Because polymer itself showed its own capacity in the charge-discharge cycling,

which can function as active material itself. When fabricating polymer electrode with LiPAA as binder



Sch.12 ) n-doping mechanism of 3,6-PPQ

It showed quite high capacity in the 1<sup>st</sup> cycle even if high irreversible capacity was shown in the 2<sup>nd</sup> cycle. It is assumed that when PPQ lithiated, catechol binded with Li ion is very stable form, when delithiated Li ion may not be released from Li-polymer alloy.

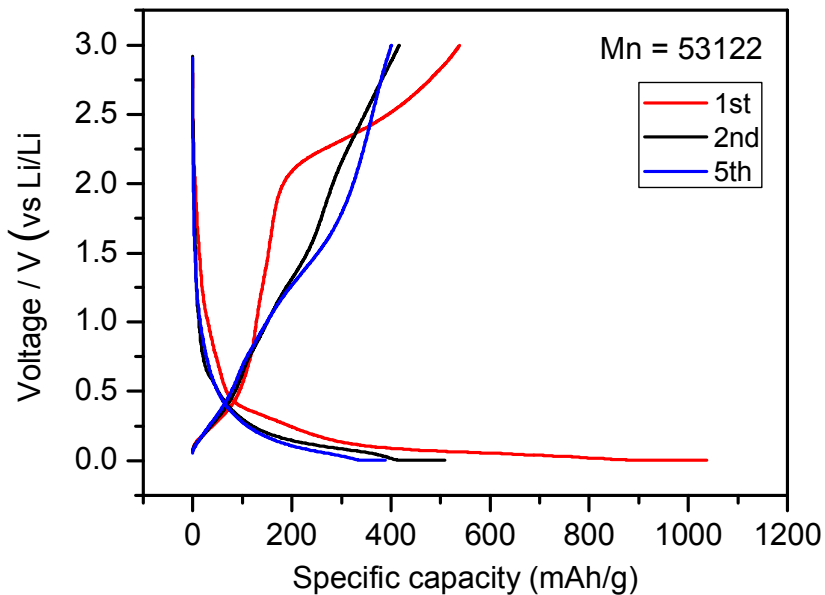
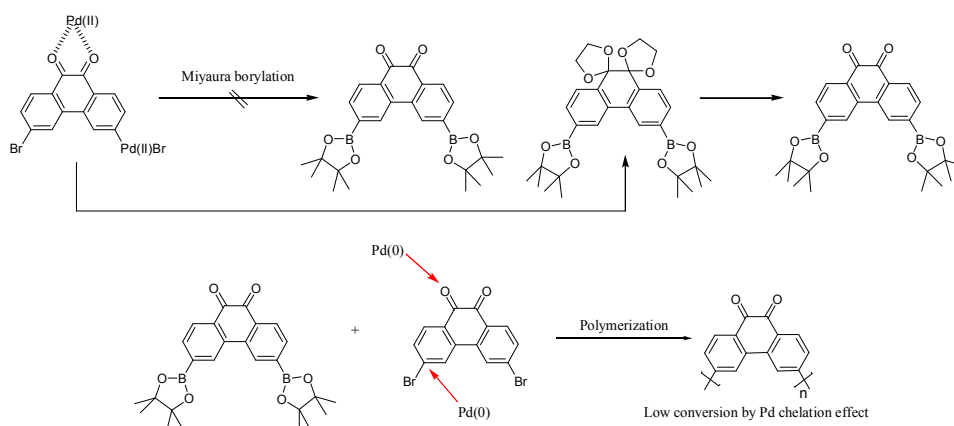


Fig.8 ) Evidence of mixed conductor of 3,6-PPQ



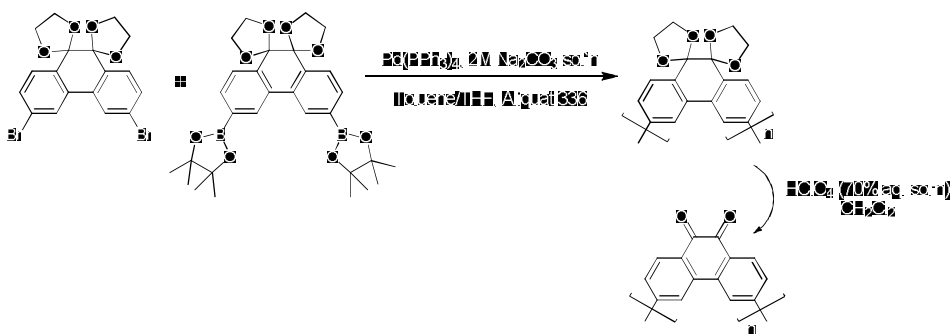
## 2.4. Modified synthetic scheme of 3,6-PPQ

However, unexpectedly, MW did not seem to be controlled by reaction time. In the middle of considering several factors about controlling MW, we thought of Pd catalyst as polymerization inhibitor.<sup>[21]</sup> Apparently, Pd(0) can form complexation with the  $\alpha$ -quinone while competing with the oxidative addition step (C-Br) although this hypothesis is yet to be proved. In the process of introducing boronic acid ester in dihaloquinone compound, Pd catalyst also may compete two reactive site, which resulted in the no reaction same as experimental result. Likewise, in the polymerization step, Pd also may inhibit polymerization by competition



Sch.13 ) The effect of Pd catalyst in polymerization and borylation

between two sites. So we modified polymerization scheme like below. Previously, deprotection was conducted prior to polymerization. However, in the modified step, polymerization was conducted prior to deprotection



Sch.14 ) Modified polymerization scheme

step because of removing the effect of Pd catalyst complexing with  $\alpha$ -quinone. So we conducted polymerization with acetal protected monomers. polymer deprotection step was troublesome in early days. Fortunately, through some trials , ethylene glycol group was nearly removed under condition, Entry 3, which was determined by by 600 NMR in pyridine-d5.

	Acid	Solvent	Time	Temp	Result
Entry 1	HClO <sub>4</sub> (70 % sol'n)	DCM	1 h	RT	Partially deprotected
Entry 2		-	5 h		Partially deprotected
Entry 3		-	17h		100 % Deprotected

Table 5. ) Screening of modification of polymer

Finally, we synthesized several polymers under various reaction time when concentration fixed . The GPC results showed average molecular

Time	Concentration (M)		Mn / PDI	C-rate test	Cycle test
1 day	0.012	Entry 1	n.a. (<5000)	O	O
		Entry 2	n.a. (<5000)		
2 days	0.012	Entry 1	109762 / 2.04	O	O
		Entry 2	88134 / 1.45	O	O
3 days	0.012	Entry 1	285910 / 1.54	O	O
		Entry 3	310235 / 1.78		

n.a. = GPC analysis peak did not appear

Table 6. ) GPC results of polymers

weight tend to increase as reaction time became longer. Generally, The degree of polymerization is dependent on the reation time which support out GPC results. Molecular weight seemed to have linearity compared to previous synthetic scheme. So we conducted to investigate electrochemical properties of samples.

## 2.5. Electrochemical test with synthesized PPQ

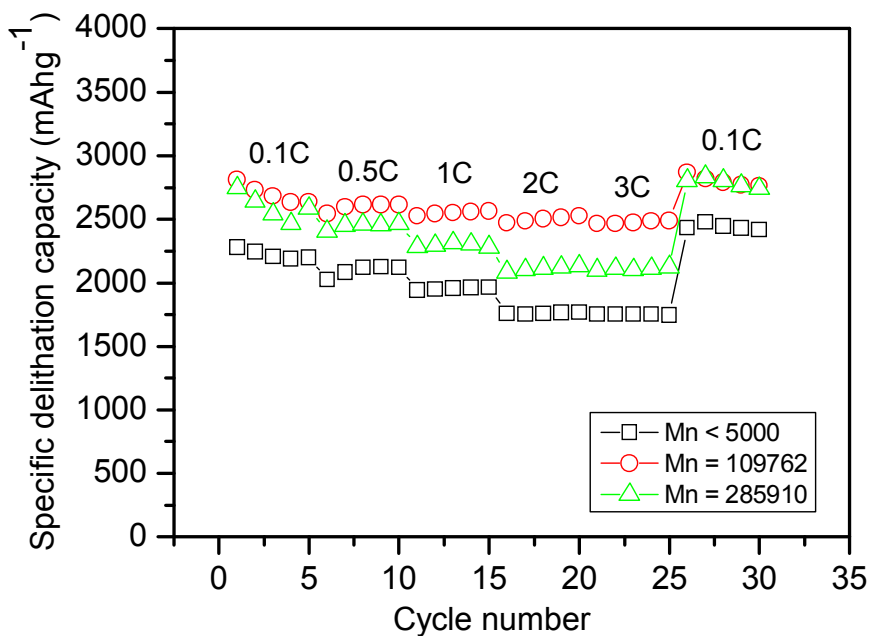


Fig 9. ) Rate capability test of Si electrode

We thought MW could be higher as reaction time became longer. At the same time conducting nature of polymer would be enhanced by band theory. And for exact investigation of binder conducting property, we used nano sized silicon particle which means minimize the volume changes during cyclings. Thus, we prepared Si electrode with synthesized polymer as binder without conducting additives and fabricated 2032 type cell for investigating the electrochemical performances. At first we conducted rate capability test of Si electrode to evaluate the conducting nature of PPQ

Expectedly, the rate capability test tell us high MW ( $> 109000$ ) polymer showed better initial capacity than polymer ( $< 5000$ ). Additionally, polymer(109000) show good rate performance at the high discharge rate.

So we assume that 2 days for synthesizing binder is a optimal reaction condition.

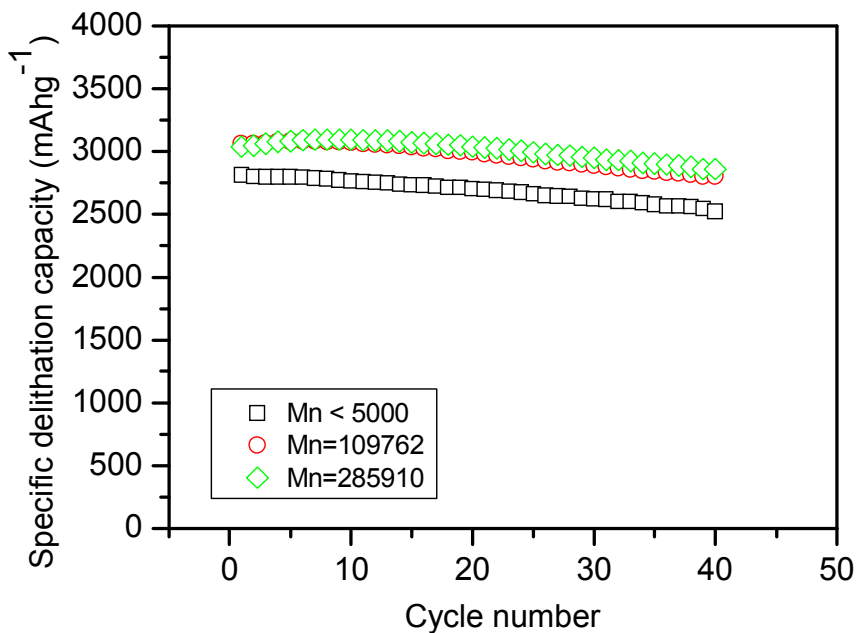


Fig 10. ) Cycle life test of Si electrode

Next in the cycle life test, cell used with high molecular polymer showed better capacity and cyclic performance than low molecular polymer . Similar to rate capability test, High molecular weight polymer has enhanced conductivity due to long conjugation length.

	1 <sup>st</sup> delithiation Capacity	Retention ratio at 40 <sup>th</sup> cycle
1 day	2813 mAh/g	89 %
2 days	3059 mAh/g	91 %
3 days	3037 mAh/g	94 %

Table 7. ) The result of cycle life test

So we think as polymer become high molecular weight, conductivity become enhanced. As a result of that, we could prove this theory when applying electrochemical system. Furthermore, we think the content of polymer binder is also important. Because even if same cyclic performances can be shown with decreased binder contents, it would be

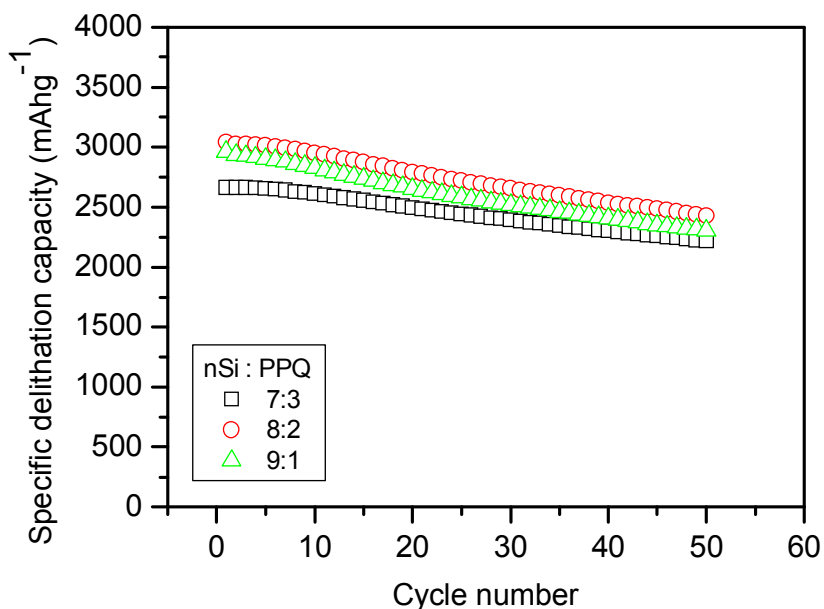


Fig 11. ) Binder contents test

Si : polymer	Retention ratio at 50 <sup>th</sup> cycle (%)
7:3	90 %
8:2	80 %
9:1	78 %

Table 8. ) The result of binder contents test

more effective. We used Si:binder as 7:3 ratio in previous studies. But we investigated cyclic performances with changing binder contents. In the case of 7:3 showed best cyclic performances. So we thought that binder contents also affect electrode integrity which result in cycling performances. So 7:3 ratio is optimal ratio and further studies is needed for decreasing binder contents.

# Experimental

## 1. The preparation of synthesis of monomers and polymers

All experimental glassware, syringes, and magnetic stirring bars were oven-dried at 120 °C for at least 4 hours and stored in desiccator until use. Air or moisture sensitive reactions were conducted under Ar atmosphere. The reactions were checked by thin layer chromatography plate mostly with using Hex:EA=2:1 eluent solution. Analytical thin layer chromatography (TLC) was performed by using Merck 60 F254 glass plates pre-coated with a 0.25-mm thickness of silica gel and then monitored under UV light (254 nm) and visualized with molybdenum staining solution. Column chromatography was performed on silica gel 60 (70 ~ 230 mesh).

<sup>1</sup>H and <sup>13</sup>C NMR spectra were measured at 400 MHz / 600 MHz and 100 MHz respectively using CDCl<sub>3</sub>, pyridine as a solvent on a Bruker Avance III spectrometer. And data were reported as follows in ppm ( $\delta$ ) from the internal standard (TMS, 0.0 ppm): chemical shift (multiplicity, integration, coupling constant in Hz). Gel permeation chromatography (GPC) analysis against poly(methyl methacrylate) standards was performed in DMF on Ultimate 3000 GPC with an LPG-3400SD pump, Shodex KD-801 columns and Refracto Max 520, a refractive index



detector. Mass spectra were recorded on JEOL, JMS-600W (Mass System), Agilent 6890 (GC System) with electron ionization mode. Elemental analysis was quantitatively recorded with Dynamic Flash Combustion method on Flash 1112.

## 2. The preparation of reagents and solvents

Materials for synthesis of PPQ were purchased from commercial suppliers used without further purification except solvents. Tetrahydrofuran (THF), 1,4-dioxane, toluene, and methanol were purchased from Daejung Chemicals & Metals. THF was distilled in the presence of sodium with benzophenone and 1,4-dioxane, toluene in the presence of calcium hydride under N<sub>2</sub> atmosphere. 9,10-Phenanthrenequinone (95 %), dibenzoyl peroxide (75 % remainder water), ethylene glycol (99+ %, extra pure), DL-10-camphorsulfonic acid (98 %), and bis(pinacolato)diboron (98 %) were purchased from Acros Organics.

[1,1'-Bis(diphenylphosphino)ferrocene]dichloropalladium(II)

(Pd(dppf)Cl<sub>2</sub>) was purchased from Sigma-Aldrich. Nitrobenzene and bromine (> 99.9 %) were purchased from Junsei Chemical. Potassium acetate (KOAc, 97 %) and sodium carbonate were purchased from Samchun Chemical. Tetrakis(triphenylphosphine)palladium(0) (> 97.0 %) and trioctylmethylammonium Chloride (R=C<sub>8</sub>-C<sub>10</sub>) as a phase-transfer

catalyst were purchased from TCI.

### **3. Fabrication of the electrodes**

Nano-sized Si powder (crystalline, APS  $\leq$  50 nm, 98 %, laser synthesized from vapor phase) was purchased from Alfa Aesar. Poly(acrylic acid) (PAA, average Mw  $\sim$  450,000), lithium hydroxide monohydrate (LiOH, ACS reagent,  $\geq$  98.0 %) and *N*-methyl-2-pyrrolidone (NMP, anhydrous, 99.5 %) were purchased from Sigma-Aldrich. 1 M LiPF<sub>6</sub> dissolved in EC/DEC (1:1 by volume) and 1.3 M LiPF<sub>6</sub> dissolved in EC/FEC/DEC (2:2:6 by volume) as electrolytes were provided from Panax Etec. PAA lithium salt (LiPAA) binder solution was made by mixing of PAA and equivalent amount of lithium hydroxide monohydrate to moles of carboxylic acid group in PAA. Concentration of LiPAA solution was 5 wt. %.

### **4. Electrode and cell preparation**

For the preparation of PPQ electrode, PPQ powder dispersed with super p and LiPAA solution dissolved in NMP was coated onto Cu foil and dried at 120 °C. The working electrodes were made by punching with a diameter of 11 mm and dried again at 120 °C overnight under vacuum oven. For the

preparation of LiPAA and PPQ as Si electrode binder, nano-sized Si powder was used and Silicon powder were dispersed with PPQ binder by using stirring bar on the magnetic stirrer. Their weight ratio was 7:3.

To check their electrochemical properties, 2032 coin-type electrode cells were fabricated with each composite (as working electrodes), lithium foil (as a counter electrode), and PP/PE/PP tri-layer separator. For the electrolyte of PPQ electrode, 1 M LiPF<sub>6</sub> dissolved in EC/DEC (1:1 by volume) was used and for the Si electrode 1.3 M LiPF<sub>6</sub> dissolved in EC/FEC/DEC (2:2:6 by volume). The cells were assembled in a glove box filled with Ar.

## 5. Electrochemical characterization methods

The galvanostatic charge-discharge cycling was conducted with WBCS3000 cycler at room temperature. The cycling mode was constant current-constant voltage (CC-CV). The cutoff-voltages of the cell with the PPQ and the Si electrodes were 5 mV ~ 3 V (*vs.* Li/Li<sup>+</sup>) and 5 mV ~ 1 V, respectively. Applied current of the cell with PPQ electrode was 50 mA g<sup>-1</sup> and cutoff-current was 25 mA g<sup>-1</sup>. For the cycling of cell with the Si electrodes, applied current was 100 mA g<sup>-1</sup> for the first cycle, 200 mA g<sup>-1</sup> for the second cycle, and respectively. The cutoff-current was 10 mA g<sup>-1</sup>. The first and second cycle as pre-cycling seemed to be very important for

forming SEI layer Si electrode. For the rate capability test, de-lithiation current applied was changed from 0.1 C to 3 C and 0.5C to 5C after pre-cycling but lithiation current applied was fix to 0.1 C and 0.5 C. The rate capability test conducted by CC charge-discharge cycling. For the cycle life test, same precycling condition was applied in the first and second cycle. Delithiation current was applied 0.1C and 1C respectively from third cycle.

## 6. Synthetic procedures for monomers and polymers

### 3,6-dibromophenanthrene-9,10-dione (**1**)

9,10-Phenanthrenequinone (4 g, 19.2 mmol) was placed in a round flask and nitrobenzene (30 ml) was added and benzoyl peroxide (0.05eq, 0.15g) and bromine (5 eq, 5 ml) was added and the reaction mixture was heated under reflux at 120 °C for 15~16 hours with Na<sub>2</sub>SO<sub>3</sub> trap apparatus. After cooling the reaction mixture, precipitated solid could be filtered and the washed out with EtOH or MeOH. Further purification could be conducted through recrystallization from xylene to give **1** as a yellowish solid (82 %): <sup>1</sup>H NMR (400 MHz, CDCl<sub>3</sub>) δ = 8.12 (d, 2H), 8.07 (d, 2H), 7.67 (dd, 2H); <sup>13</sup>C NMR (CDCl<sub>3</sub>, 100 MHz): δ = 178.8, 135.9, 133.4, 132.1, 129.8, 127.4; HRMS (EI-MS) calcd for C<sub>14</sub>H<sub>6</sub>Br<sub>2</sub>O<sub>2</sub> 365.871, found 365.872

### **3,6-dibromo-9,10-bis(hexyloxy)phenanthrene (2)**

Prepared compound **1** (2 g, 5.46 mmol), was dissolved in THF / H<sub>2</sub>O =2:1 (volumic ratio) and Na<sub>2</sub>S<sub>2</sub>O<sub>4</sub> (4.75 g, 27.3 mmol) and TBAB (0.88 g, 2.73 mmol) was added in the solution at rt. Reaction mixture became quite green solution and checked reduction product by TLC monitoring. After 30 min, K<sub>2</sub>CO<sub>3</sub> (11.3 g, 81.9 mmol) and hexylbromide (4.6 ml, 32.7 mmol) was added and heated at 80 °C overnight. After cooling, crude mixture was extracted with DCM and dried with MgSO<sub>4</sub> and concentrated rotary evaporator. Further purification was conducted with silica gel column chromatography (Hexane:DCM = 4:1 → 2:1) to give **2** as a white solid (70 %): <sup>1</sup>H NMR (400 MHz, CDCl<sub>3</sub>) δ= 8.64 (d, 2H), 8.09 (d, 2H), 7.70 (dd, 2H), 4.15, 4.17 (t, 4H), 1.91 ~ 1.84 (m, 4H), 1.56 ~ 1.51 (m, 4H), 1.39 ~ 1.35 (m, 8H), 0.94 ~ 0.90 (m, 6H); <sup>13</sup>C NMR (CDCl<sub>3</sub>, 100 MHz): 143.1, 130.4, 128.8, 128.7, 125.3, 124.2, 120.3, 73.7, 31.6, 30.3, 25.8, 22.6, 13.9

### **3,6-dibromo-9,10-bis(octyloxy)phenanthrene (3)**

Same procedure was conducted as compound **2**. Bromooctane was used as alkyl halide (65 %): <sup>1</sup>H NMR (400 MHz, CDCl<sub>3</sub>) δ= 8.64 (d, 2H), 8.09 (d, 2H), 7.70 (dd, 2H), 4.15, 4.17 (t, 4H), 1.91 ~ 1.84 (m, 4H), 1.56 ~ 1.51 (m, 4H), 1.39 ~ 1.35 (m, 8H), 0.94 ~ 0.90 (m, 6H); <sup>13</sup>C NMR (CDCl<sub>3</sub>, 100

MHz):  $\delta$  = 143.1, 130.4, 128.8, 128.7, 125.39, 124.2, 120.3, 73.7, 31.8, 30.4, 29.4, 29.3, 26.2, 22.6, 14.1

**2,2'-(9,10-bis(hexyloxy)phenanthrene-3,6-diyl)bis(4,4,5,5 tetramethyl-1,3,2-dioxaborolane) (4)**

Compound **2** (1g, 1.86 mmol) was dissolved in 1,4-dioxane and Pd(dppf)Cl<sub>2</sub> (0.068 g, 0.093 mmol), bis(pinacolato)diboron (1.18 g, 4.65 mmol) and KOAc (1.13g, 11.16 mmol) was added to solution. The reaction mixture was heated under reflux for 17 hours with TLC monitoring. After cooling, crude was extracted with Ethyl acetate and concentrated with rotary evaporator. Purification was conducted with silica gel chromatography (Hexane:EtOAc = 16:1 → 8:1 → 4:1) and obtained **4** as yellowish solid (42 %) <sup>1</sup>H NMR (400 MHz, CDCl<sub>3</sub>)  $\delta$ = 9.21 (d, 2H), 8.23 (d, 2H), 8.02 (dd, 2H), 4.21 (t, 4H), 1.93 (m, 4H), 1.56 (m, 8H), 1.42 (s, 24H), 1.39 (m, 4H), 0.93 (m, 6H)

**2,2'-(9,10-bis(octyloxy)phenanthrene-3,6-diyl)bis(4,4,5,5-tetramethyl-1,3,2-dioxaborolane) (5)**

Same procedure was conducted as compound **4**. Compound **4** was used as starting material (50 %): <sup>1</sup>H NMR (400 MHz, CDCl<sub>3</sub>)  $\delta$ = 9.22 (d, 2H), 8.23 (d, 2H), 8.03 (dd, 2H), 4.21 (t, 4H), 1.91 (m, 4H), 1.56 (m, 4H), 1.43 (s, 24H), 1.38 (m, 8H), 0.91 (m, 6H)

### **Poly(9,10-bis(hexyloxy)phenanthrene (6)**

Compound **2** was dissolved in 1,4-dioxane and compound **4**, Pd(PPh<sub>3</sub>)<sub>4</sub> and 2M Na<sub>2</sub>CO<sub>3</sub> sol'n was added in the reaction mixture. Reaction mixture was heated 100°C for 15 h. After cooling, after which the resulting polymer was precipitated in methanol. The precipitate was filtered and subsequently fractionated by Soxhlet extraction with chloroform. The chloroform solution, containing the higher molar mass fraction, was concentrated in vacuum. GPC was measured in THF PS standard and the results were in manuscript part.

### **Poly((9,10-bis(hexyloxy)phenanthrene-co-9,9-dioctylfluorene)) (7)**

Same procedure was applied to the synthesis of this polymer. 9,9-dioctylfluorene was used instead of compound **4**. GPC was measured in THF PS standard and the results were in manuscript part.

### **Poly(9,10-bis(octyloxy)phenanthrene-co-phenanthrene-9,10-dione)) (8)**

Same procedure was applied to the synthesis of this polymer. Compound **1** was used instead of compound **4**. GPC was measured in THF PS standard and the results were in manuscript part.

### **3,6-dibromophenanthrene-9,10-di(ethyleneglycol)ketal (9)**

3,6-dibromophenanthrenequinone(1.00 g, 2.73 mmol) in pressure tube was added to methanol (15ml) and (±)-camphorsulfonic acid(0.82g, 0.3 eq) and ethylene glycol(4.57ml, 81.9 mmol) were added to reaction mixture and heated at 120 °C for 12 hours. After 12 hours, reaction mixture was converted to white color and cooled to room temperature. Crude mixture was filtered and washed with diethyl ether to produce **9** as a white solid (90 %): <sup>1</sup>H NMR (400 MHz, CDCl<sub>3</sub>) δ = 7.96 (s, 2H), 7.62 (d, 2H), 7.56 (d, 2H), 4.16, 3.63 (br, 8H); <sup>13</sup>C NMR (CDCl<sub>3</sub>, 100 MHz): δ = 133.8, 132.2, 132.1, 128.2, 127, 124.4, 92.1, 61.3; HRMS (EI-MS) calcd for C<sub>18</sub>H<sub>14</sub>Br<sub>2</sub>O<sub>4</sub> 453.923, found 453.922

**3,6-bis(4,4,5,5-tetramethyl-1,3,2-dioxaborolan-2-yl)phenanthrene 9,10-di(ethyleneglycol)ketal (10)**

compound **9** (2.00 g, 4.40 mmol) was dissolved in distilled 1,4-dioxane(150ml) and Pd(dppf)Cl<sub>2</sub> (0.1eq, 0.32 g), bis(pinacolato)diboron (2.4g, 2.1 mmol) and KOAc (2.59g, 6 eq) was added to solution. The reaction mixture was heated under reflux for 17 hours under Ar atmosphere. After cooling, crude was filtered with Cellite with DCM and Ethyl acetate. This organic solution was concentrated by rotary evaporator and obtained crude was purified with silica gel column chromatography (Hexane:EtOAc = 8:1 → 4:1 → 2:1). Further purification of obtained crude was conducted with washing EtOH several times to produce **10** as a



white solid (42 %):  $^1\text{H}$  NMR (400 MHz,  $\text{CDCl}_3$ )  $\delta$  8.41 (s, 2H), 7.87 (d, 2H), 7.74 (d, 2H), 4.15, 3.67 (br, 8H), 1.35 (s, 24H);  $^{13}\text{C}$  NMR ( $\text{CDCl}_3$ , 100 MHz):  $\delta$  = 135.5, 135.1, 132.5, 130.4, 125.3, 92.6, 84, 61.3, 24.8; HRMS (EI-MS) calcd for  $\text{C}_{30}\text{H}_{38}\text{O}_8\text{B}_2$  548.275, found 548.274

### **3,6-bis(4,4,5,5-tetramethyl-1,3,2-dioxaborolan-2-yl)phenanthrene 9,10-dione(11)**

compound **10** (1.94g, 3.53 eq) was dissolved in DCM(120ml) and perchloric acid 70% solution (2.5ml, 10 eq.) was added to solution. The reaction mixture was stirred vigorously for 1 hour at room temperature. Reaction crude was quenched by aq. $\text{NaHCO}_3$  and the organic layer was dried over  $\text{MgSO}_4$ , filtered and concentrated by rotary evaporator. The obtained product was purified by washing with EtOH to produce **11** as an orange powder (58 %):  $^1\text{H}$  NMR (400 MHz,  $\text{CDCl}_3$ )  $\delta$ = 8.52 (s, 2H), 8.16 (d, 2H), 7.89 (d, 2H), 1.42 (s, 24H);  $^{13}\text{C}$  NMR ( $\text{CDCl}_3$ , 100 MHz)  $\delta$  = 180.8, 135.6, 135, 132.5, 130.3, 84.6, 24.9; HRMS (EI-MS) calcd for  $\text{C}_{26}\text{H}_{38}\text{O}_6\text{B}_2$  460.222, found 460.222

### **3,6-polyphenanthrenequinone (3,6-PPQ) (12)**

A solution of compound **1** (0.5 g, 1.52 mmol) and **11** (0.7 g, 1.52 mmol) in Toluene (80 mL) and THF (20 ml) was stirred in round flask. Then,  $\text{Pd}(\text{PPh}_3)_4$  (15.6 mg, 0.15 mmol),  $\text{Na}_2\text{CO}_3$  (2.0 mL, 2.0 M in distilled

water) and Aliquat 336 several drops were added. The reaction mixture was stirred for 2 days at 110 °C, after which the resulting crude mixture was concentrated by rotary evaporator and precipitated in methanol / H<sub>2</sub>O / 1N HCl. The precipitate was centrifuged and dried in air for some time. Subsequently dried polymer was fractionated by Soxhlet extraction with methanol and dichloromethane. Residue deep brownish solid was collected and dried vacuum pump. GPC was measured in DMF PMMA standard and the results were in manuscript part.

### **3,6-polyphenanthrene-9,10-di(ethyleneglycol)ketal (13)**

compound **9** (0.55 g, 1.21 mmol) and compound **10** (0.66g, 1.21 mmol) in Toluene and THF was stirred in round flask. Then, Pd(PPh<sub>3</sub>)<sub>4</sub> (0.14 g, 0.12 mmol), and Na<sub>2</sub>CO<sub>3</sub> (8.0 mL, 2.0 M in distilled water) were added. The reaction mixture was stirred vigorously for various time and under concentration at 110 °C, after which the resulting crude mixture was concentrated by rotary evaporator and precipitated in methanol : H<sub>2</sub>O = 1:1 (V/V) . The precipitate was centrifuged and dried in air for some time. And subsequent procedure is same as compound **12**. Obtained product is gray or pale gray colored powder.

### **3,6-polyphenanthrenequinone (modified pathway) (14)**

Compound **13** (0.4 g) was placed in round flask. Then HClO<sub>4</sub> 70%

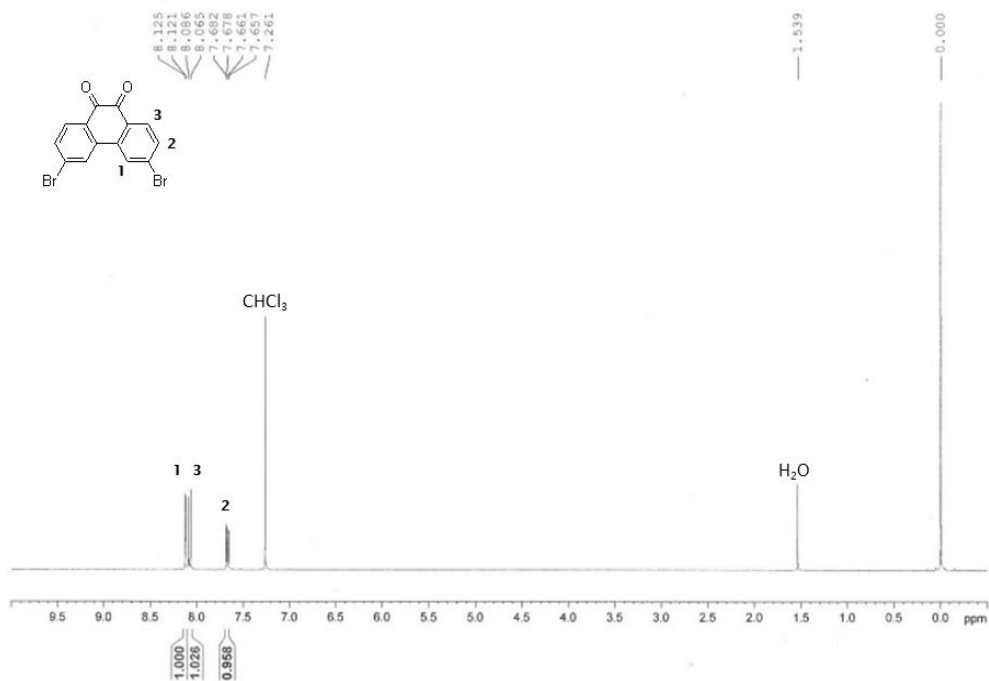
solution was added to flask and reaction mixture was stirred vigorously. After 15 ~ 16 h, this mixture was filtered and washed out with H<sub>2</sub>O, DCM and acetone . residue solid was collected and dried to give **14** as deep brown powder.

# Appendix

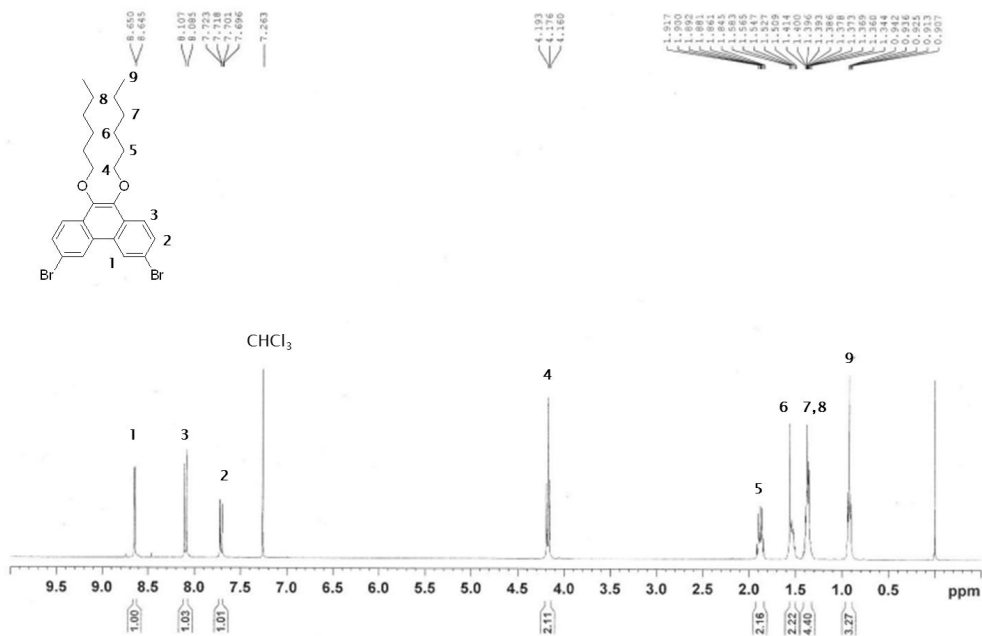
## List of $^1\text{H}$ NMR spectra of selected compound

1. 400 MHz  $^1\text{H}$  NMR spectra ( $\text{CHCl}_3$ -*d*) of compound **1**
2. 400 MHz  $^1\text{H}$  NMR spectra ( $\text{CHCl}_3$ -*d*) of compound **2**
3. 400 MHz  $^1\text{H}$  NMR spectra ( $\text{CHCl}_3$ -*d*) of compound **3**
4. 400 MHz  $^1\text{H}$  NMR spectra ( $\text{CHCl}_3$ -*d*) of compound **4**
5. 400 MHz  $^1\text{H}$  NMR spectra ( $\text{CHCl}_3$ -*d*) of compound **5**
6. 400 MHz  $^1\text{H}$  NMR spectra ( $\text{CHCl}_3$ -*d*) of compound **6**
7. 400 MHz  $^1\text{H}$  NMR spectra ( $\text{CHCl}_3$ -*d*) of compound **7**
8. 400 MHz  $^1\text{H}$  NMR spectra ( $\text{CHCl}_3$ -*d*) of compound **8**
9. 400 MHz  $^1\text{H}$  NMR spectra ( $\text{CHCl}_3$ -*d*) of compound **9**
10. 400 MHz  $^1\text{H}$  NMR spectra ( $\text{CHCl}_3$ -*d*) of compound **10**
11. 400 MHz  $^1\text{H}$  NMR spectra ( $\text{CHCl}_3$ -*d*) of compound **11**
12. 400 MHz  $^1\text{H}$  NMR spectra ( $\text{DMSO-}d_6$ ) of compound **12**
13. 400 MHz  $^1\text{H}$  NMR spectra (pyridine-*d*<sub>5</sub>) of compound **13**
14. 400 MHz  $^1\text{H}$  NMR spectra (pyridine-*d*<sub>5</sub>) of compound **14**

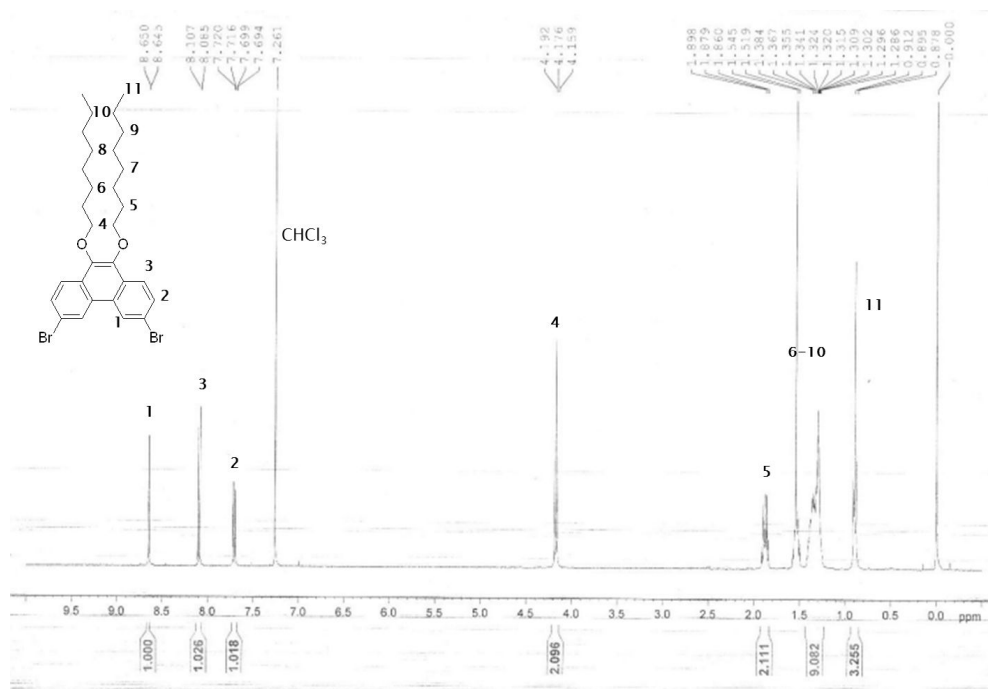
# 1. 400 MHz $^1\text{H}$ NMR spectra ( $\text{CHCl}_3-d$ ) of compound 1



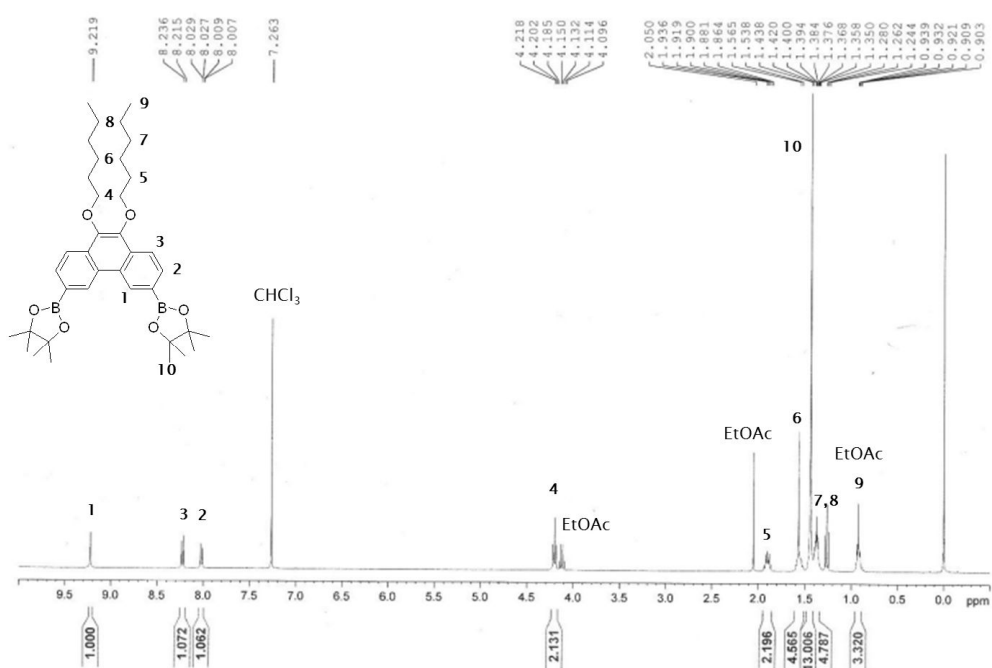
# 2. 400 MHz $^1\text{H}$ NMR spectra ( $\text{CHCl}_3-d$ ) of compound 2



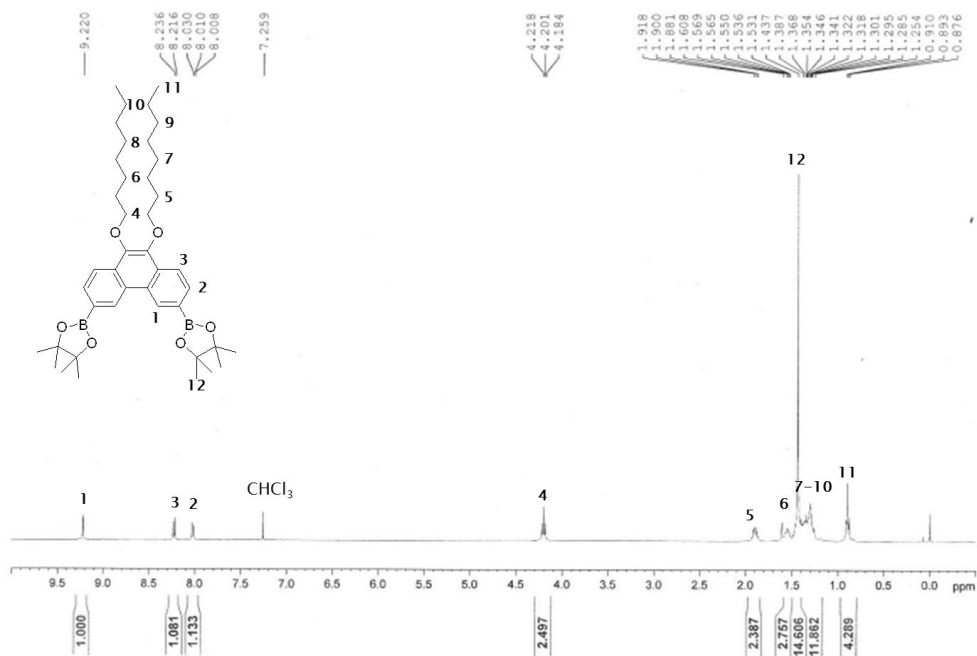
### 3. 400 MHz $^1\text{H}$ NMR spectra ( $\text{CHCl}_3$ -*d*) of compound 3



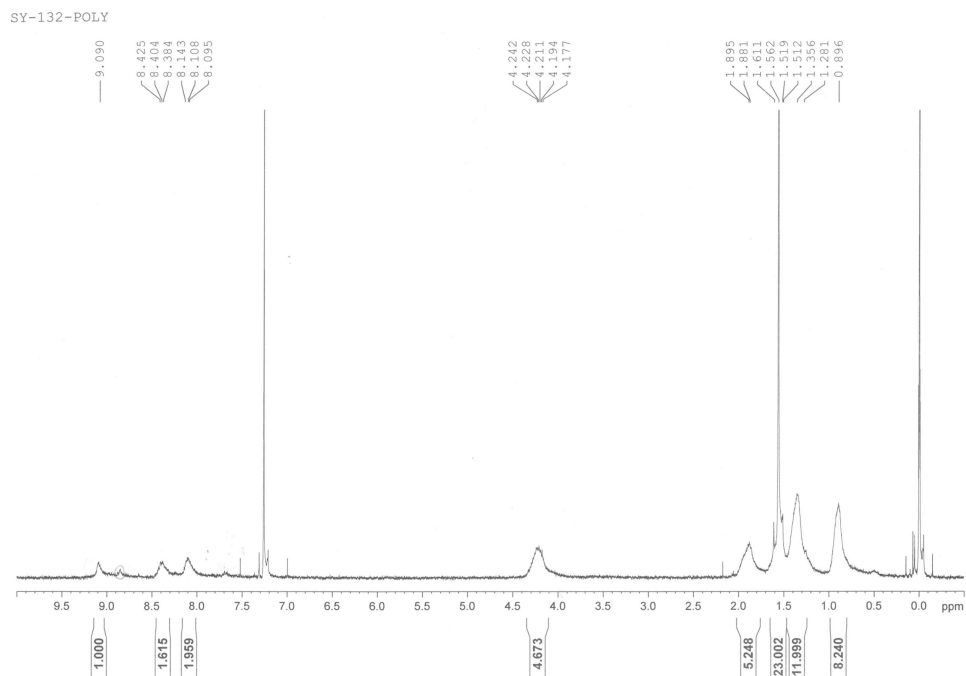
### 4. 400 MHz $^1\text{H}$ NMR spectra ( $\text{CHCl}_3$ -*d*) of compound 4



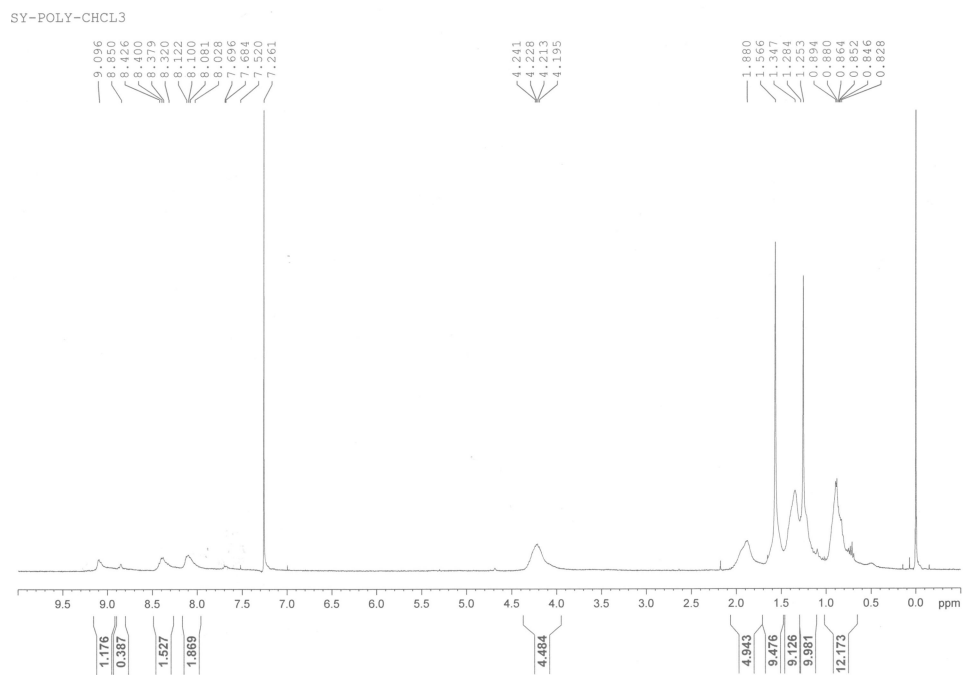
5. 400 MHz  $^1\text{H}$  NMR spectra ( $\text{CHCl}_3-d$ ) of compound **5**



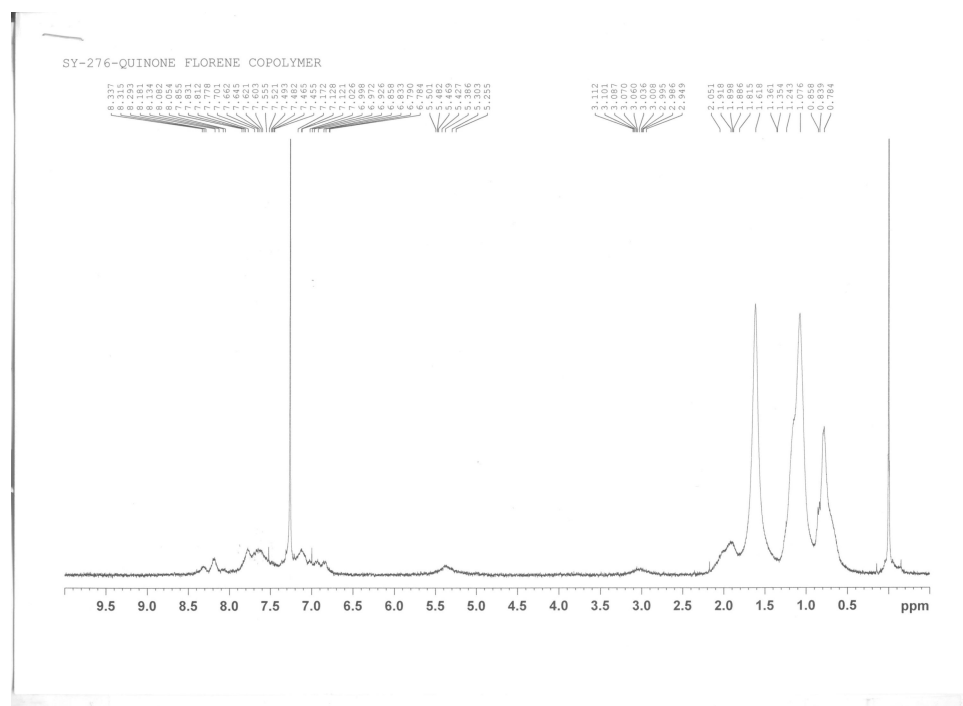
6. 400 MHz  $^1\text{H}$  NMR spectra ( $\text{CHCl}_3-d$ ) of compound **6**



## 7. 400 MHz $^1\text{H}$ NMR spectra ( $\text{CHCl}_3-d$ ) of compound **7**

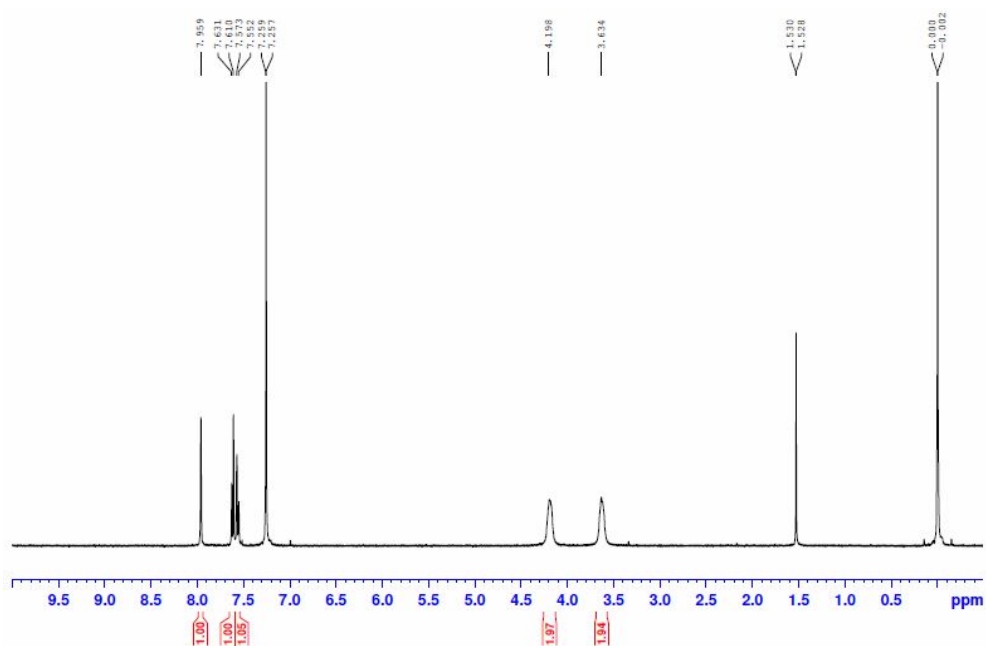


## 8. 400 MHz $^1\text{H}$ NMR spectra ( $\text{CHCl}_3-d$ ) of compound **8**

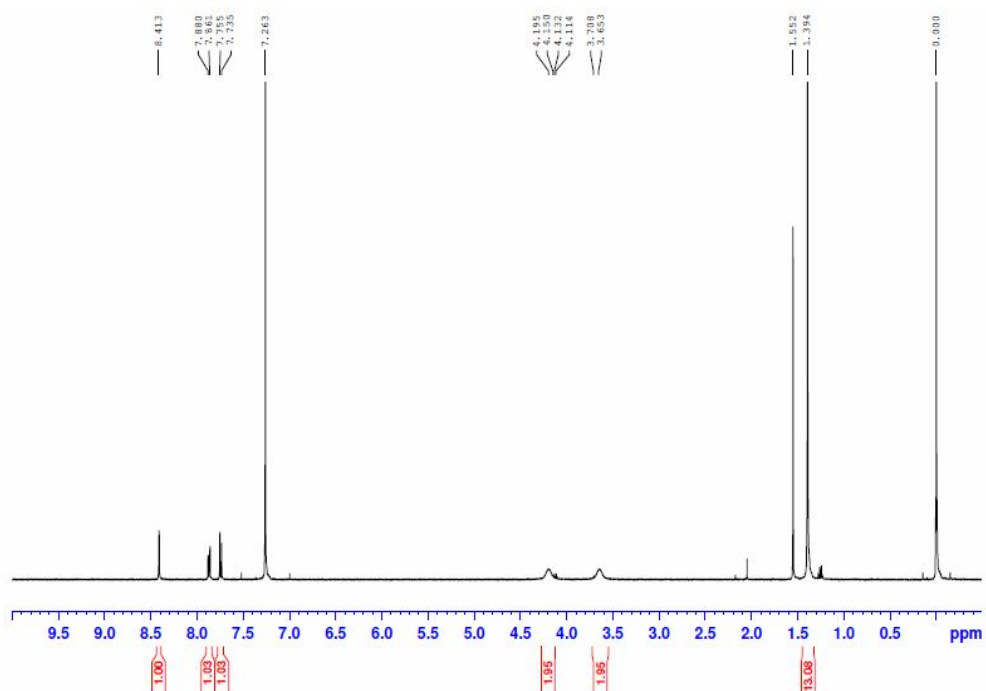




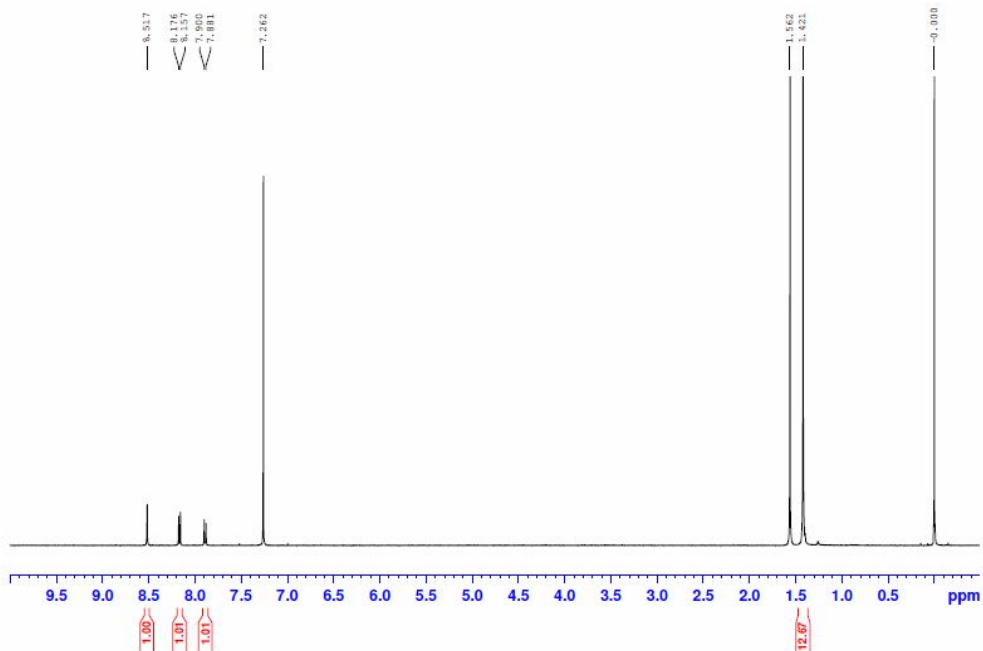
9. 400 MHz  $^1\text{H}$  NMR spectra ( $\text{CHCl}_3-d$ ) of compound **9**



10. 400 MHz  $^1\text{H}$  NMR spectra ( $\text{CHCl}_3-d$ ) of compound **10**

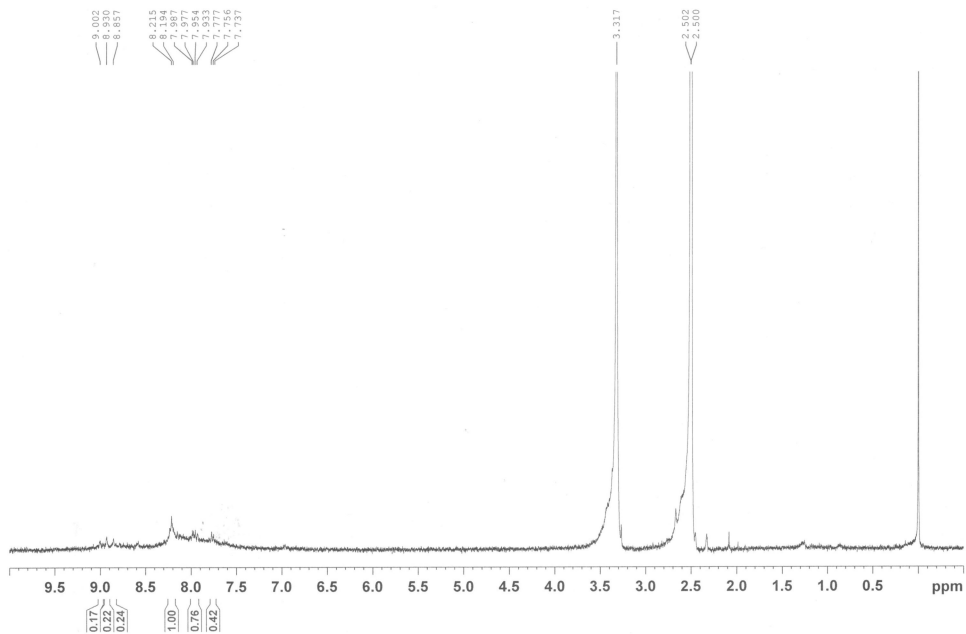


## 11. 400 MHz $^1\text{H}$ NMR spectra ( $\text{CHCl}_3-d$ ) of compound **11**

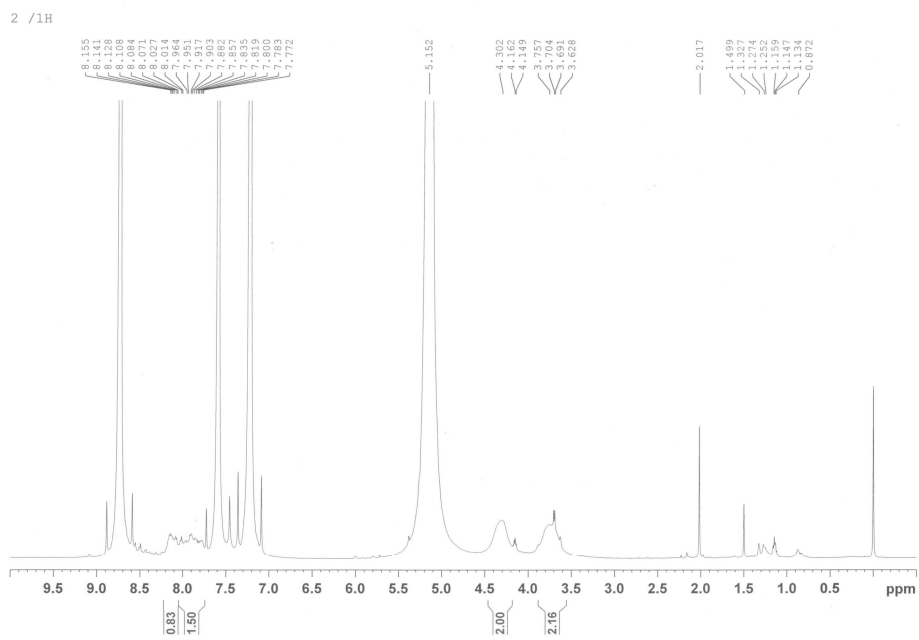


## 12. 400 MHz $^1\text{H}$ NMR spectra ( $\text{DMSO}-d_6$ ) of compound **12**

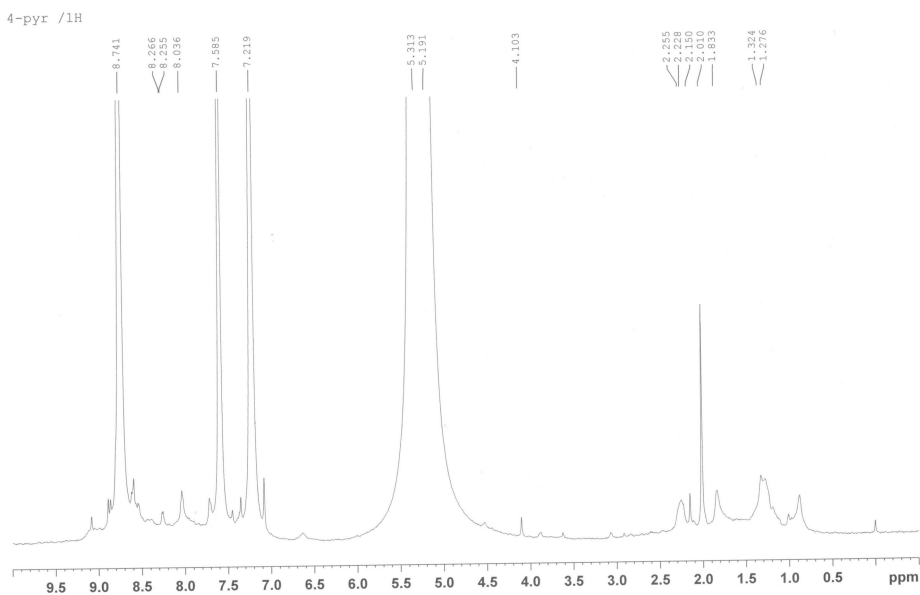
SY-238-POLY-DMSO



### 13. 400 MHz $^1\text{H}$ NMR spectra (pyridine- $d_5$ ) of compound 13



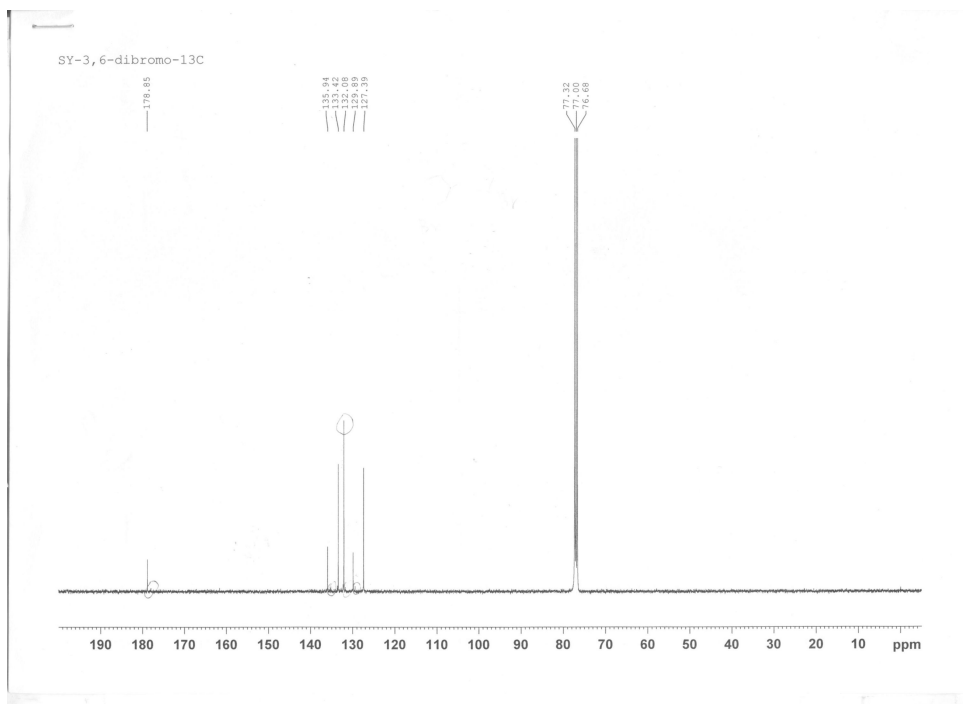
### 13. 400 MHz $^1\text{H}$ NMR spectra (pyridine- $d_5$ ) of compound 13



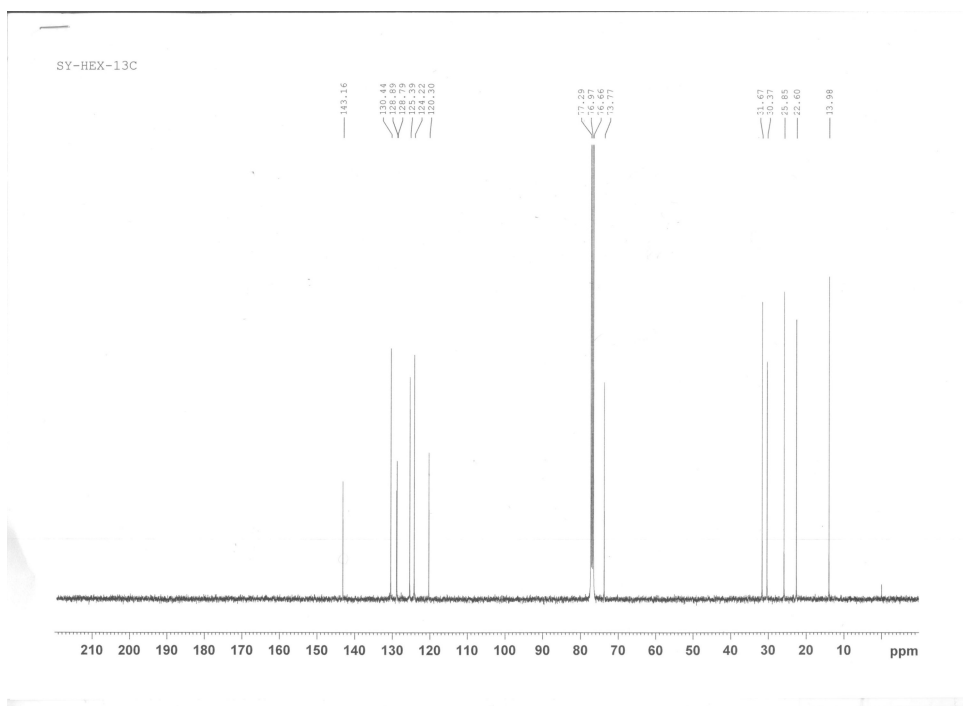
## List of $^{13}\text{C}$ NMR spectra of selected compound

1. 100 MHz  $^{13}\text{C}$  NMR spectra ( $\text{CHCl}_3$ -*d*) of compound **1**
2. 100 MHz  $^{13}\text{C}$  NMR spectra ( $\text{CHCl}_3$ -*d*) of compound **2**
3. 100 MHz  $^{13}\text{C}$  NMR spectra ( $\text{CHCl}_3$ -*d*) of compound **3**
4. 100 MHz  $^{13}\text{C}$  NMR spectra ( $\text{CHCl}_3$ -*d*) of compound **9**
5. 100 MHz  $^{13}\text{C}$  NMR spectra ( $\text{CHCl}_3$ -*d*) of compound **10**
6. 100 MHz  $^{13}\text{C}$  NMR spectra ( $\text{CHCl}_3$ -*d*) of compound **11**

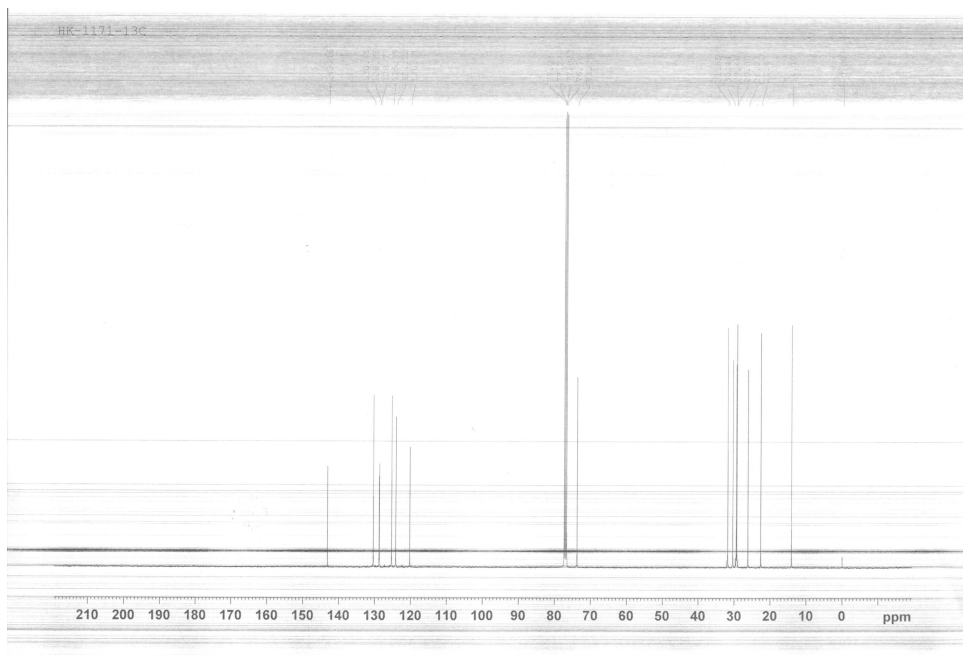
## 1. 100 MHz $^{13}\text{C}$ NMR spectra ( $\text{CHCl}_3-d$ ) of compound 1



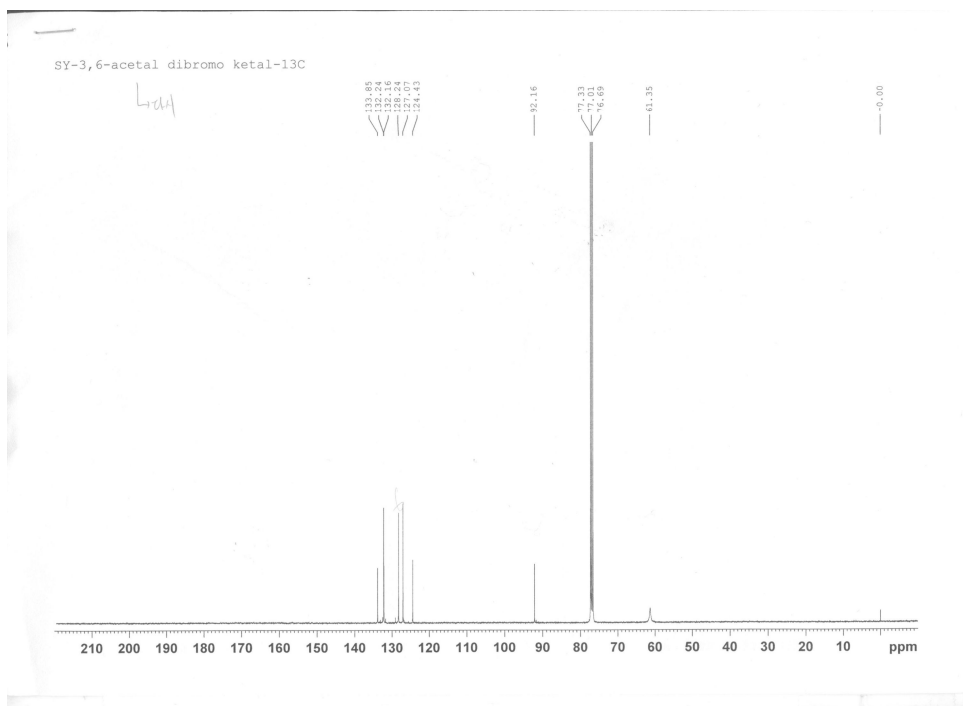
## 2. 100 MHz $^{13}\text{C}$ NMR spectra ( $\text{CHCl}_3-d$ ) of compound 2



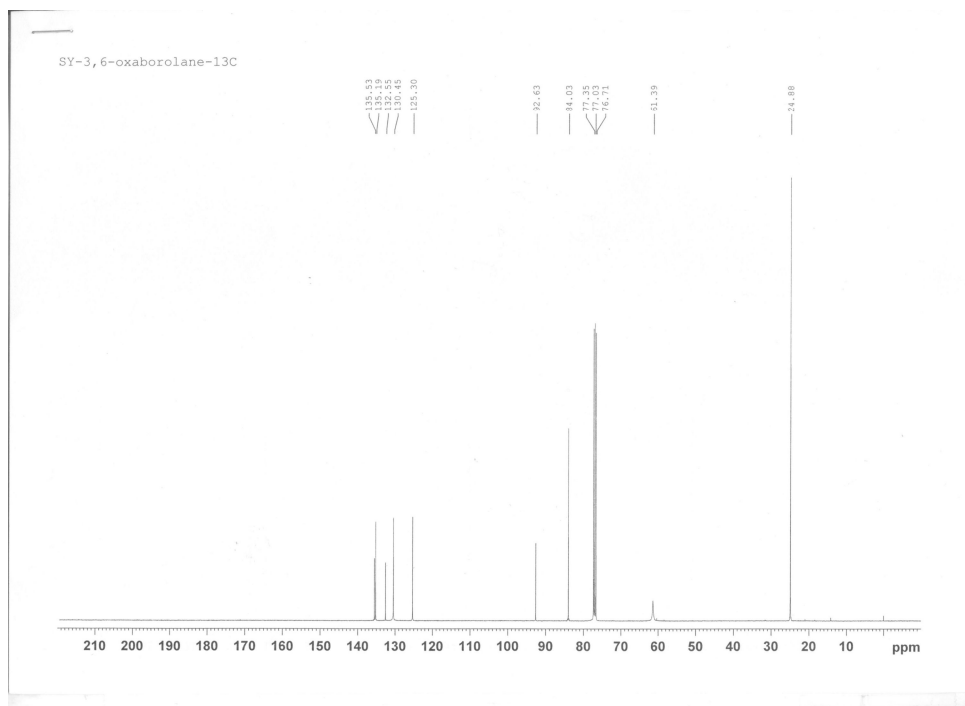
3. 100 MHz  $^{13}\text{C}$  NMR spectra ( $\text{CHCl}_3\text{-}d$ ) of compound 3



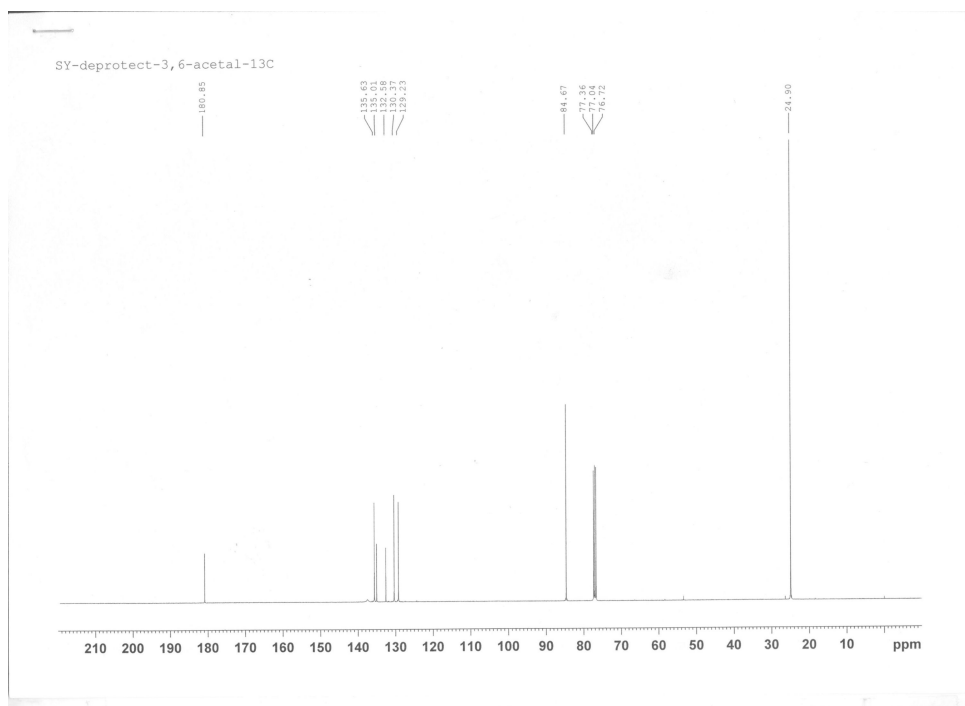
4. 100 MHz  $^{13}\text{C}$  NMR spectra ( $\text{CHCl}_3\text{-}d$ ) of compound 9



5. 100 MHz  $^{13}\text{C}$  NMR spectra ( $\text{CHCl}_3-d$ ) of compound **10**



6. 100 MHz  $^{13}\text{C}$  NMR spectra ( $\text{CHCl}_3-d$ ) of compound **11**



## REFERENCES

- [1] Whittingham, M.S. Electrical energy storage and intercalation chemistry. *Science*, **1976**, *192*,
- [2] Whittingham, M.S. Materials challenges facing electrical energy storage. *MRS Bull.* **2008**, *33*
- [3] Shinichi Komaba, Keiji Shimomura, Naoaki Yabuuchi, Tomoaki Ozeki, Hiroharu Yui, and Kohzo Konno *J. Phys. Chem. C*, **2011**, *115*, 13487–13495
- [4] M. N. Obrovacz and Leif Christensen, *Electrochemical and Solid-State Letters*, **2004**, A93-A96
- [5] Uday Kasavajjula a, Chunsheng Wang a, A. John Appleby b, *Journal of Power Sources* ,*163*,**2007**, 1003–1039
- [5] Shidi Xun, Xiangyun Song, Vincent Battaglia, Gao Liu, *Journal of The Electrochemical Society*, **2013**, A849-A855



- [6] Ji Heon Ryu, Jae Woo Kim, Yung-Eun Sung, and Seung M. Oh, *Electrochemical and Solid-State Letters*, **2004**, A306-A309
- [7] Li, H.; Huang, X.; Chen, L.; Wu, Z, *Electrochem. Solid-State Lett.* **1999**, 2, 547–549.
- [8] Kovalenko, I.; Zdyrko, B.; Magasinski, A.; Hertzberg, B.; Milicev, Z.; Burtovyy, R.; Luzinov, I.; Yushin, *Science*, **2011**, 334, 75–79.
- [9] a) G. Liu, S. Xun, N. Vukmirovic, X. Song, P. Olalde-Velasco, H. Zheng, V. S. Battaglia, L. Wang, W. Yang, *Adv. Mater.* **2011**, 23, 4679-4683; b) M. Wu, X. Xiao, N. Vukmirovic, S. Xun, P. K. Das, X. Song, P. Olalde-Velasco, D. Wang, A. Z. Weber, L.-W. Wang, V. S. Battaglia, W. Yang, G. Liu, *J. Am. Chem. Soc.* **2013**.
- [10] Z. Chen, L. Christensen, J.R. Dahn, *Electrochemistry Communications*, **2003**, 919.
- [11] J. Li, R.B. Lewis, J.R. Dahn, *Electrochemical and Solid-State Letters* , **2007**, A17.
- [12] Yamamoto, T., Hayashi, Y., Yamamoto, Y. *Bull. Chem. Soc. Jpn.*, **1978**, 51, 2091.

[13] (a) Miyaura, N., Yamada, K., and Suzuki, A., *Tetrahedron Lett.* **1979**, 3437; (b) Miyaura, N. and Suzuki, A. *J. Chem. Soc. Chem. Commun.*, **1979** 866;

[14] Liu, C., Repolev, A., and Zhou, B., *J. Polym. Sci., Part A: Polym. Chem.* **2008**, 46, 7268.

[15] a) M. V. Bhatt, *Tetrahedron* **1964**, 20, 803-821; b) K. Brunner, A. van Dijken, H. Börner, J. J. A. M. Bastiaansen, N. M. M. Kiggen, B. M. W. Langeveld, *J. Am. Chem. Soc.* **2004**, 126, 6035-6042

[16] Wouter Vanormelingen, Alfons Smeets, Edith Franz, Inge Asselberghs, Koen Clays, Thierry Verbiest, and Guy Koeckelberghs, *Macromolecules* **2009**, 42, 4282–4287

[17] a) T. Ishiyama, M. Murata, N. Miyaura, *The Journal of Organic Chemistry* **1995**, 60, 7508-7510; b) T. Lee, C. A. Landis, B. M. Dhar, B. J. Jung, J. Sun, A. Sarjeant, H.-J. Lee, H. E. Katz, *J. Am. Chem. Soc.* **2009**, 131, 1692-1705.

[18] a) C. Yang, H. Scheiber, E. J. W. List, J. Jacob, K. Müllen, *Macromolecules* **2006**, 39, 5213-5221;

[19] Muddasir Hanif, LU Ping, GU Cheng, WANG Zhi-ming, YANG Shu-min, YANG Bing, WANG Chun-lei and MA Yu-guang, *CHEM. RES. CHINESE UNIVERSITIES*, **2009**, 25(6), 950—956

[20] a) Yasuhiro Shirai, Andrew J. Osgood, Yuming Zhao, Yuxing Yao, Lionel Saudan, Hanbiao Yang, Chiu Yu-Hung, Lawrence B. Alemany, Takashi Sasaki, Jean-François Morin, Jason M. Guerrero, Kevin F. Kelly, and James M. Tour, *J. AM. CHEM. SOC.* **2006**, 128, 4854 – 4864; b) R. Mondal, S. Ko, E. Verploegen, H. A. Becerril, M. F. Toney, Z. Bao, *J. Mater. Chem.* **2011**, 21, 1537-1543.

[21] a) Leandro A. Estrada and Douglas C. Neckers, *Org. Lett.*, **2011**, 13, 3304–3307; b) Ciszek, J. W.; Tour, J. M. *Tetrahedron Lett.* **2004**, 45, 2801; c) Estrada, L. A.; Neckers, D. C. *J. Org. Chem.* **2009**, 74, 8484-8487

## Abstract in Korean

최근 고용량 고출력이 요구되는 전기자동차 전력저장장치등 차세대 리튬이온 배터리의 수요가 증가해왔다. 이런 추세에 따라서 이론용량이 큰 실리콘이 급부상하게 되면서 많은 연구가 진행되어 왔다 하지만 실리콘의 상업화를 위한 많은 노력에도 불구하고 현재까지도 아직 탄소계 음극에서 벗어나지 못하고 있다. 실리콘의 경우 충방전시 매우 큰 부피변화가 일어나고 이에 활물질의 파쇄 이로 인한 전지용량의 감소로 전지로서는 가장 큰 단점을 지니고 있다. 지난연구에서는 활물질의 변화(나노구조화, 충전재와의 결합등)에 주로 초점을 맞추었지만, 최근 바인더가 cyclic performance를 향상시켜줄수 있다는 보고가 많이 되어 오고 있다. 따라서 바인더의 선택이 고용량의 음극을 도입하는데 매우 중요하다고 할수 있겠다. 그래서 우리 실험실에서는 전도성을 가지는 새로운 고분자 바인더를 개발하였다. 바인더가 도전재의 역할도 하게 된다면 우리는 통상적으로 사용하였던 도전재를 사용할 필요없이 단지 바인더만으로 전지의 성능을 유지할수 있다. 또한 소량의 바인더를 사용하더라도 전기화학적인 성능을 유지시켜 줄수 있을거라고 예상하였다. 이에 새로운바인더 물질로 3,6-poly(phenanthrenequinone)을 목표물질로 선정하고 이것을 스즈키 커플링 반응에 기반하여 성공적으로 합성할 수가 있었다. 합성된 고분자를 통해 여러 전기화학적인 특성을 조사해보았다. 고분자만을 활물질로 한 전지를 만들어 충방전 실험을 한결과 고분자가 리튬가

전자를 동시에 받을수 있는 mixed conductor로서 작용하여 활물질로서 용량발현을 할수 있다는 것을 확인할 수가 있었습니다. 그리고 좀더 높은 분자량의 고분자를 합성하기 위해 분자량을 컨트롤 할수 있는 원인을 규명하고 그에 고분자량의 고분자를 합성할수 있었다. 합성된 고분자를 통해 전기화학적인 특성을 분석해본결과 속도특성실험에서는 올리고머 수준의 분자들보다 분자량이 높은 고분자의 경우 초기용량이 더 높게 나왔고 약 100000인 경우의 고분자가 가장 좋은 속도 특성을 나타내었다. 그리고 수명특성실험의 경우에도 더 높은 고분자의 경우 좋은 수명특성을 보여 고분자의 전도성이 분자량과 관련이 있음을 알수 있었고 높은 분자량의 고분자의 경우 더 향상된 전도성으로 인해 더 좋은 전기화학적 성능 발현을 한것으로 생각된다. 결국 새롭게 합성된 고분자는 기존에 쓰던 도전재의 사용없이도 실리콘전극의 도입이 가능하기 때문에 앞으로 바인더로서 가능성있는 물질로 보인다.

학번 : 2012-20981